

**ISTANBUL TECHNICAL UNIVERSITY ★ GRADUATE SCHOOL OF SCIENCE**  
**ENGINEERING AND TECHNOLOGY**

**EFFECT OF PROMOTERS ON ACTIVATED CARBON SUPPORTED Fe  
CATALYST FOR LIGHT OLEFINS PRODUCTION via FISCHER-TROPSCH  
SYNTHESIS**



**M.Sc. THESIS**

**Melis KIRARSLAN**

**Department of Chemical Engineering**

**Chemical Engineering Programme**

**DECEMBER 2019**



**ISTANBUL TECHNICAL UNIVERSITY ★ GRADUATE SCHOOL OF SCIENCE**  
**ENGINEERING AND TECHNOLOGY**

**EFFECT OF PROMOTERS ON ACTIVATED CARBON SUPPORTED Fe  
CATALYST FOR LIGHT OLEFINS PRODUCTION via FISCHER-TROPSCH  
SYNTHESIS**

**M.Sc. THESIS**

**Melis KIRARSLAN  
(506171028)**

**Department of Chemical Engineering**

**Chemical Engineering Programme**

**Thesis Advisor: Asst. Prof. Dr. Gamze GÜMÜŞLÜ GÜR  
Thesis Co-Advisor: Dr. Gamze BEHMENYAR**

**DECEMBER 2019**



**İSTANBUL TEKNİK ÜNİVERSİTESİ ★ FEN BİLİMLERİ ENSTİTÜSÜ**

**FISHER-TROPSCH SENTEZİYLE HAFİF OLEFİN ÜRETİMİNDE AKTİF  
KARBON DESTEKLİ Fe KATALİZÖRÜ ÜZERİNDE PROMOTÖR ETKİSİ**

**YÜKSEK LİSANS TEZİ**

**Melis KIRARSLAN  
(506171028)**

**Kimya Mühendisliği Anabilim Dalı**

**Kimya Mühendisliği Programı**

**Tez Danışmanı: Dr. Öğr. Üyesi Gamze GÜMÜŞLÜ GÜR  
Eş Danışman: Dr. Gamze BEHMENYAR**

**ARALIK 2019**



Melis KIRARSLAN, a M. Sc. student of ITU Graduate School of Science Engineering and Technology student ID 506171028, successfully defended the thesis entitled “EFFECT OF PROMOTERS ON ACTIVATED CARBON SUPPORTED Fe CATALYST FOR LIGHT OLEFINS PRODUCTION via FISCHER-TROPSCH SYNTHESIS”, which she prepared after fulfilling the requirements specified in the associated legislations, before the jury whose signatures are below.

**Thesis Advisor:** **Asst. Prof. Dr. Gamze GÜMÜŞLÜ GÜR** .....  
Istanbul Technical University

**Co-Advisor:** **Dr. Gamze BEHMENYAR** .....  
TUBITAK MRC

**Jury Members :** **Prof. Dr. Hüsnü ATAKÜL** .....  
Istanbul Technical University

**Prof. Dr. Hasancan OKUTAN** .....  
Istanbul Technical University

**Assoc. Prof. Alper SARIOĞLAN** .....  
TUBITAK MRC

**Date of Submission : 15 November 2019**  
**Date of Defense : 16 December 2019**







*To my family,*



## FOREWORD

I would like to offer my special thanks to Asst. Prof. Dr. Gamze GÜMÜŞLÜ GÜR, my M.Sc. advisor, guiding me with her deep knowledge and experience. I learned how to be successful from her and she helped me gain a different point of view as an engineer.

The door of Dr. Gamze BEHMENYAR, my co-adviser, office was always open whenever I ran into trouble or had a question about my research. I am gratefully indebted to her for a very valuable effort on this thesis as an engineer and as a human.

I would like to offer my thanks to Assoc. Prof. Dr. Alper SARIOĞLAN for leading the project. I would like to express my deep gratitude to Özgür Can KORKMAZ with whom we deal with challenges and exchange ideas and Özlem ATAÇ for supporting and training me in each stage of the process.

My special thanks are extended to the staff of TUBITAK MRC for their valuable technical support on this thesis. I wish to thank Hadi RAHNAMAEI ZONOUZ, Hande ÇUKURLU, Melike TUPTUP and Ayşe KAŞKA supporting and helping me while I was writing the thesis.

The important one is for my family, I am so grateful for their moral and material support all through my life.

I would like to acknowledge TUBITAK for financial and technical support for the ‘217M105- Catalyst and Reactor Development for Light Olefins Production from Cleaned Synthesis Gas’ project.

November 2019

Melis KIRARSLAN  
(Chemical Engineer)



## TABLE OF CONTENTS

	<u>Page</u>
<b>FOREWORD</b> .....	<b>ix</b>
<b>TABLE OF CONTENTS</b> .....	<b>xi</b>
<b>ABBREVIATIONS</b> .....	<b>xiii</b>
<b>LIST OF TABLES</b> .....	<b>xv</b>
<b>LIST OF FIGURES</b> .....	<b>xvii</b>
<b>SUMMARY</b> .....	<b>xix</b>
<b>ÖZET</b> .....	<b>xxi</b>
<b>1. INTRODUCTION</b> .....	<b>1</b>
1.1 Purpose of the Thesis .....	3
1.2 Thesis Plan .....	3
<b>2. LITERATURE REVIEW</b> .....	<b>5</b>
2.1 Light Olefins in Chemical Industry.....	5
2.2 Light Olefin Production Using Syngas .....	6
2.2.1 Indirect processes .....	7
2.2.2 Direct processes .....	8
2.3 Fischer-Tropsch to Olefins .....	8
2.3.1 Fischer-Tropsch synthesis .....	8
2.3.2 Fischer-Tropsch mechanism and product distribution .....	10
2.4 Fischer-Tropsch to Olefins Catalysts .....	13
2.4.1 Active metal.....	13
2.4.2 Promoters.....	14
2.4.3 Unsupported Fe catalyst .....	18
2.4.4 Supported Fe catalyst.....	18
<b>3. EXPERIMENTAL</b> .....	<b>23</b>
3.1 Materials.....	23
3.1.1 Chemical materials .....	23
3.1.2 Gases and liquids .....	23
3.2 Catalyst Synthesis .....	24
3.2.1 Sequential impregnation .....	24
3.2.2 Co-impregnation .....	25
3.3 Catalyst Characterization .....	27
3.4 High Throughput Screening System .....	29
3.5 Catalyst Test Procedure.....	32
3.6 Calculations .....	32
<b>4. RESULTS AND DISCUSSION</b> .....	<b>35</b>
4.1 Structural Properties of Catalysts .....	35
4.1.1 SEM-EDX .....	35
4.1.2 BET.....	37
4.1.3 XRD.....	38
4.1.4 H <sub>2</sub> -TPR .....	40
4.2 Catalytic Performance .....	42

4.2.1 Effects of temperature and pressure on catalytic activity and selectivity to light olefins.....	42
4.2.2 10Fe catalyst behavior under FTO conditions.....	43
4.2.3 Promoter effect of Mn on olefin selectivity and synthesis method effect on yield.....	44
4.2.4 Promoter effects of Mn, Zn and Cu on AC supported Fe catalyst .....	45
4.2.5 Promoter effects of Zn, K and Na on 10Fe2Mn .....	48
4.2.6 Promoter effects of Mn, K and Na on 10Fe2Zn .....	50
4.2.7 Promoter effect of Mn, Zn, K and Na on 10Fe-2Cu.....	53
4.2.8 Promoter effects of Na and S promoters on AC supported Fe catalyst ....	56
4.2.9 Comparison of 10Fe2Mn-1K, 10Fe2Zn-1K and 10Fe-2Cu-1K .....	57
<b>5. CONCLUSION.....</b>	<b>61</b>
<b>REFERENCE .....</b>	<b>63</b>
<b>CURRICULUM VITAE .....</b>	<b>69</b>



## **ABBREVIATIONS**

<b>AC</b>	: Activated Carbon
<b>ASF</b>	: Anderson-Schulz-Flory
<b>BET</b>	: Brunauer–Emmett–Teller
<b>BTL</b>	: Biomass to Liquid
<b>CTL</b>	: Coal to Liquid
<b>DME</b>	: Dimethyl ether
<b>DMTO</b>	: Dimethyl Ether to Olefins
<b>EG</b>	: Ethylene glycol
<b>FCC</b>	: Fluid Catalytic Cracking
<b>FTO</b>	: Fischer-Tropsch to Olefins
<b>FT</b>	: Fischer-Tropsch Synthesis
<b>GC</b>	: Gas Chromatography
<b>GHSV</b>	: Gas Hourly Space Velocity
<b>GTL</b>	: Gas to Liquid
<b>IWI</b>	: Incipient Wetness Impregnation
<b>MTO</b>	: Methanol to Olefin
<b>PET</b>	: Polyethylene terephthalate
<b>PMMA</b>	: Polymethyl methacrylate
<b>PVC</b>	: Polyvinyl chloride
<b>SBR</b>	: Styrene Butadiene Rubber
<b>TOS</b>	: Time on Stream
<b>XRD</b>	: X-Ray Diffraction





## LIST OF TABLES

	<u>Page</u>
<b>Table 2.1</b> : Promoters used in Fe based catalysts and their effects. ....	<b>17</b>
<b>Table 3.1</b> : Chemicals that are used for catalyst synthesis. ....	<b>23</b>
<b>Table 3.2</b> : Specification of liquids used. ....	<b>24</b>
<b>Table 3.3</b> : Specifications and applications of gases used.....	<b>24</b>
<b>Table 3.4</b> : Formulation and synthesis method of AC supported catalyst.....	<b>27</b>
<b>Table 3.5</b> : Methods and equipments used in the characterization of catalysts. ....	<b>28</b>
<b>Table 4.1</b> : Weight concentration (wt.%) of samples according to SEM-EDX. ....	<b>37</b>
<b>Table 4.2</b> : Surface area of catalysts.....	<b>37</b>
<b>Table 4.3</b> : Catalytic performance of 10Fe2Mn-1K, 10Fe2Zn-1K and 10Fe-2Cu-1K. .....	<b>60</b>



## LIST OF FIGURES

	<u>Page</u>
<b>Figure 2.1</b> : Ethylene production in the United States and Western Europe between 2010 and 2018 [19, 21].	5
<b>Figure 2.2</b> : Propylene production in the United States and Western Europe between 2010 and 2018 [19, 24].	6
<b>Figure 2.3</b> : Indirect (green) and direct (blue) processes for the production of light olefins [1].	7
<b>Figure 2.4</b> : The mechanism of Fischer-Tropsch reaction [32].	11
<b>Figure 2.5</b> : Anderson-Schulz-Flory (ASF) model [1].	12
<b>Figure 2.6</b> : Three components of a catalyst.	18
<b>Figure 3.1</b> : Sequential impregnation procedure.	25
<b>Figure 3.2</b> : Co-impregnation procedure.	26
<b>Figure 3.3</b> : 10Fe-2Cu-1K catalyst.	27
<b>Figure 3.4</b> : High Throughput System.	29
<b>Figure 3.5</b> : Process flow diagram of the high throughput system.	30
<b>Figure 3.6</b> : (a) Feed and (b) reaction parts of AMTECH software.	31
<b>Figure 3.7</b> : (a) Inside view and (b) outside view of a fixed bed reactor.	31
<b>Figure 4.1</b> : SEM-EDX images of (a) unloaded AC, (b) 10Fe, (c) 10Fe2Zn-1K, (d) 10Fe-2Cu-1K.	36
<b>Figure 4.2</b> : XRD patterns of calcined 10Fe, 10Fe-2Cu, 10Fe-2Cu-1K and 10Fe-2Cu-1Na catalysts.	38
<b>Figure 4.3</b> : XRD patterns of calcined 10Fe, 10Fe2Zn and 10Fe2Zn-1K catalysts.	39
<b>Figure 4.4</b> : XRD patterns of calcined 10Fe-2Cu-1K and after reaction 10Fe-2Cu-1K.	40
<b>Figure 4.5</b> : H <sub>2</sub> -TPR curves of 10Fe, 10Fe-2Cu, 10Fe-2Cu-1K and 10Fe2Zn-1K catalysts.	41
<b>Figure 4.6</b> : (a) CO conversion and (b) light olefins selectivity of 10Fe and 10Fe-2Mn catalysts at different reaction conditions, H <sub>2</sub> /CO = 1, GHSV=2000 h <sup>-1</sup> .	43
<b>Figure 4.7</b> : Product selectivity of 10Fe.	44
<b>Figure 4.8</b> : Light olefins yield of 10Fe-2Mn and 10Fe2Mn catalysts.	45
<b>Figure 4.9</b> : (a) CO conversion, (b) light olefins, (c) CO <sub>2</sub> and (d) CH <sub>4</sub> selectivity of Mn, Zn and Cu promoted catalysts at 340 °C, 10 bar, H <sub>2</sub> /CO = 1, GHSV=2000 h <sup>-1</sup> .	46
<b>Figure 4.10</b> : O/P ratio of Mn, Zn and Cu promoted catalysts at 340 °C, 10 bar, H <sub>2</sub> /CO = 1, GHSV=2000 h <sup>-1</sup> .	47
<b>Figure 4.11</b> : Light olefins yield of 10Fe2Mn, 10Fe2Zn and 10Fe-2Cu.	47
<b>Figure 4.12</b> : (a) CO conversion, (b) light olefins, (c) CO <sub>2</sub> and (d) CH <sub>4</sub> selectivity of promoted 10Fe2Mn catalysts at 340 °C, 10 bar, H <sub>2</sub> /CO = 1, GHSV=2000 h <sup>-1</sup> .	49
<b>Figure 4.13</b> : O/P ratio of promoted 10Fe2Mn catalysts at 340 °C, 10 bar, H <sub>2</sub> /CO = 1, GHSV=2000 h <sup>-1</sup> .	49

<b>Figure 4.14</b> : Light olefins yield of 10Fe2Mn, 10Fe2Mn-1K, 10Fe2Mn-1Na and 10Fe2Mn-2Zn. ....	<b>50</b>
<b>Figure 4.15</b> : (a) CO conversion, (b) light olefins, (c) CO <sub>2</sub> and (d) CH <sub>4</sub> selectivity of promoted 10Fe2Zn catalyst at 340 °C, 10 bar, H <sub>2</sub> /CO = 1, GHSV=2000 h <sup>-1</sup> . ....	<b>51</b>
<b>Figure 4.16</b> : O/P ratio of promoted 10Fe2Zn catalysts at 340 °C, 10 bar, H <sub>2</sub> /CO = 1, GHSV=2000 h <sup>-1</sup> . ....	<b>52</b>
<b>Figure 4.17</b> : Light olefins yield of 10Fe2Zn, 10Fe2Zn-2Mn, 10Fe2Zn-1K and 10Fe2Zn-1Na. ....	<b>52</b>
<b>Figure 4.18</b> : (a) CO conversion, (b) light olefins, (c) CO <sub>2</sub> and (d) CH <sub>4</sub> selectivity of promoted 10Fe-2Cu catalysts at 340 °C, 10 bar, H <sub>2</sub> /CO = 1, GHSV=2000 h <sup>-1</sup> . ....	<b>54</b>
<b>Figure 4.19</b> : O/P ratio of promoted 10Fe-2Cu catalysts at 340 °C, 10 bar, H <sub>2</sub> /CO = 1, GHSV=2000 h <sup>-1</sup> . ....	<b>55</b>
<b>Figure 4.20</b> : Light olefins yield of 10Fe-2Cu, 10Fe-2Cu-1K, 10Fe-2Cu-1Na, 10Fe-2Cu-2Mn, 10Fe-2Cu-2Zn. ....	<b>55</b>
<b>Figure 4.21</b> : (a) CO conversion and (b) light olefins selectivity of 10Fe0.3Na0.1S at 340 °C, 10 bar, H <sub>2</sub> /CO = 1, GHSV=2000 h <sup>-1</sup> . ....	<b>56</b>
<b>Figure 4.22</b> : O/P ratio of 10Fe0.3Na0.1S catalyst at 340 °C, 10 bar, H <sub>2</sub> /CO = 1, GHSV=2000 h <sup>-1</sup> . ....	<b>57</b>
<b>Figure 4.23</b> : (a) CO conversion, (b) light olefins, (c) CO <sub>2</sub> and (d) CH <sub>4</sub> selectivity of K promoted Mn, Zn and Cu catalysts at 340 °C, 10 bar, H <sub>2</sub> /CO = 1, GHSV=2000 h <sup>-1</sup> . ....	<b>58</b>
<b>Figure 4.24</b> : O/P ratio of K promoted Mn, Zn and Cu catalysts at 340 °C, 10 bar, H <sub>2</sub> /CO = 1, GHSV=2000 h <sup>-1</sup> . ....	<b>58</b>
<b>Figure 4.25</b> : Light olefins yield of 10Fe2Mn-1K, 10Fe2Zn-1K and 10Fe-2Cu-1K. ....	<b>59</b>

# **EFFECT OF PROMOTERS ON ACTIVATED CARBON SUPPORTED Fe CATALYST FOR LIGHT OLEFINS PRODUCTION via FISCHER-TROPSCH SYNTHESIS**

## **SUMMARY**

Olefins, also known as alkenes, are hydrocarbons belonging to organic compounds. Ethylene (C<sub>2</sub>H<sub>4</sub>), propylene (C<sub>3</sub>H<sub>6</sub>) and butylene (C<sub>4</sub>H<sub>8</sub>), are called light olefins and building blocks of the chemical industry. These hydrocarbons are the main feedstock of many materials used in modern life. Ethylene is among the most produced chemicals in the world and plays a leading role in the production of a wide range of products, from packaging to clothing. Demand for light olefins is expected to increase further due to the increase in world population and living standards.

Light olefins are obtained by cracking of commercially available petroleum product naphtha. Due to the rapid depletion of oil reserves, alternative processes for the production of light olefins have begun to be explored. Fischer-Tropsch (FT) synthesis which is used for production of hydrocarbons can be an alternative way to produce light olefins from syngas (CO and H<sub>2</sub>). This process, which produces olefins directly from syngas, is called 'Fischer-Tropsch to Olefins (FTO)'. FTO process needs to be developed for the production of valuable chemicals for countries with limited oil but large reserves of coal, biomass or natural gas. In this context, Turkey's lignite which has lower calorific value is a proper feedstock to produce syngas by gasification and syngas can be used to produce light olefins.

Main parameters that affect the product distribution of FTO reaction are temperature, pressure, gas composition and flow. Also, catalyst plays very important role for FTO. High CO conversion and high selectivity to light olefins are main expectations from the catalysts. In addition, selectivity to CO<sub>2</sub>, methane, paraffin and higher molecular weight hydrocarbon products are expected to be lower.

A wide variety of catalysts have been investigated for selective light olefins production in literature. Different active metals, promoters and support materials were tested. But, lower catalytic activity, deactivation of the catalyst in a short time, coke formation, high carbon number products were problems which researchers have encountered.

In this work, 16 Fe based activated carbon supported catalysts with promoters and without promoters were synthesized by employing incipient wetness impregnation. Effect of Mn, Zn, K, Na, Cu and S promoters were investigated separately and in groups. Samples were characterized by Scanning Electron Microscope Energy Dispersive X-ray (SEM-EDX), Brunauer-Emmett-Teller (BET), X-Ray Diffraction (XRD), H<sub>2</sub>-Temperature Programmed Reduction (H<sub>2</sub>-TPR) to find out the physical and structural properties of the catalysts.

Catalysts were tested in high pressure and throughput test system for 160 h. First, different temperatures and pressures were applied to decide the optimum reaction conditions. Results of tests on 10Fe and 10Fe-2Mn catalysts showed that 340 °C, 10

bar and  $H_2/CO = 1$  were the optimum conditions for activity and light olefins selectivity.

The effect of the preparation method was investigated with the sequential (10Fe-2Mn) and co-impregnated Mn promoter (10Fe2Mn). Mn was loaded (2 wt.% wrt. catalyst) into the AC supported Fe catalysts. The co-impregnated catalyst has a higher olefin yield. This has been associated with co-impregnated catalyst exposed to less heat treatment thus sintering of iron particles was prevented.

Comparing the promoters Mn (10Fe2Mn), Zn (10Fe2Zn), and Cu (10Fe-2Cu); Mn enhanced the O/P ratio (2.0) whereas Zn improved the CO conversion (65%). The Cu promoted catalyst had the lowest  $CO_2$  selectivity with a value of 25%.

Zn, K and Na promoters were added to 10Fe2Mn catalyst by sequential impregnation and their effects were investigated. Na and K promoter helped both increase CO conversion and stability of it. The addition of promoters had no significant effect on olefin selectivity. The highest O/P ratio of 4.3 was obtained with 10Fe2Mn-1K catalyst but it reached stability at 2.4 after 160 hours.

Mn, K and Na promoters were added by sequential impregnation to 10Fe2Zn catalyst. The addition of K and Na had no negative effect on the conversion. Mn was the promoter which most lowers the activity of 10FeZn catalyst. The light olefins selectivity of catalysts added with Mn, K, and Na (10Fe2Zn-2Mn, 10Fe2Zn-1K, and 10Fe2Zn-1Na) was similar and greater than the light olefins selectivity of 10Fe2Zn catalyst. Addition of K increased olefin selectivity and decreased  $CH_4$  selectivity. O/P ratio of 10Fe2Zn-1K catalyst started at high value of 5.6 and reached 2.7 at the end of the reaction.

Mn, Zn, K and Na promoters were added to the 10Fe-2Cu catalyst by sequential impregnation. The addition of K and Na decreased  $CH_4$  selectivity. K and Na promoted catalysts had the higher olefin selectivity (c.a. 27%) and lower  $CH_4$  selectivity (<10%) than other catalysts. Cu and K promoted 10Fe-2Cu-1K exhibited the highest O/P ratio among all other catalysts. O/P ratio reached 6.3 at the initial period of the reaction. Then, it started to decline slightly until it became 3.8 after the 160 h reaction. But still, it had the highest O/P ratio.

Na and S promoted 10Fe0.3Na0.1S catalyst was synthesized by co-impregnation method. The light olefins selectivity decreased from 20 to 18% which was lower than the expected value and the O/P ratio was 2.0. This may be attributed to low  $H_2/CO$  ratio at high temperature test.

10Fe2Mn-1K, 10Fe2Zn-1K and 10Fe-2Cu-1K catalysts which were the best ones in their groups were compared. CO conversion of 10Fe2Zn-1K catalyst was the highest. The conversion of the Cu-containing catalyst started at a higher value, indicating that Cu improves the reduction of iron. 10Fe2Mn-1K catalyst had the lowest olefin selectivity and highest  $CH_4$  selectivity. When the O/P ratio was considered, Cu-K combination had the best result and Zn-K followed it.

The light olefins yield of catalysts were also calculated. After 160 hours reaction, 10Fe2Zn-1K catalyst reached the highest olefin yield with a value of  $3.4 \times 10^{-3} \text{ g}_C / \text{g}_{Fe.S}$ .

According to all test results, 10Fe2Zn-1K and 10Fe-2Cu-1K catalysts could be promising choices for FTO reaction industrially.

# **FISHER-TROPSCH SENTEZİYLE HAFİF OLEFİN ÜRETİMİNDE AKTİF KARBON DESTEKLİ Fe KATALİZÖRÜ ÜZERİNDE PROMOTÖR ETKİSİ**

## **ÖZET**

Olefinler diğeri ismiyle alkenler organik bileşikler ailesine ait hidrokarbonlardır. Hafif olefin olarak adlandırılan etilen ( $C_2H_4$ ), propilen ( $C_3H_6$ ) ve bütilen ( $C_4H_8$ ) kimya endüstrisinin yapı taşlarıdır ve modern hayatta kullanılan birçok malzeme bu hidrokarbonlardan oluşmaktadır. Örneğin etilen dünyada en çok üretilen kimyasallar arasındadır ve paketlenmeden giyime kadar geniş yelpazedeki ürünlerin üretimlerinde başrol oynamaktadır. Artan dünya nüfusu ve yaşam standartları sebebiyle hafif olefinlere talebin daha da artacağı düşünülmektedir.

Hafif olefinler ticari olarak petrol ürünü olan naftanın parçalanması ile elde edilmektedir. Petrol rezervlerinin hızla azalması sebebiyle hafif olefin üretimi için alternatif prosesler araştırılmaya başlanmıştır. Fischer-Tropsch sentezi de ürün dağılımına bakıldığında hafif olefin üretimi için verimli olabilecek bir prostedir. Kömür ya da biyokütlenin gazlaştırılmasından elde edilen sentez gazından ( $CO$  ve  $H_2$ ) sıvı yakıt üretimi için kullanılan FTS, uygun katalizörler eşliğinde hafif olefin eldesi için de kullanılabilir. Sentez gazından direkt olarak olefin üretilen bu proses ise 'Fischer-Tropsch to Olefins, (FTO)' olarak adlandırılır. Petrol rezervleri sınırlı; kömür, biyokütle ya da doğal gaz rezervi geniş olan ülkeler için bu proses değerli kimyasalların üretimi için geliştirilmelidir. Bu bağlamda, Türkiye'nin ısı değeri düşük linyit kömürünü kullanarak gazlaştırma yoluyla sentez gazı elde edilmesi ve bu sentez gazından FTO ile hafif olefinlerin üretimi amaçlanmaktadır.

FTO reaksiyonu için sıcaklık, basınç, gaz kompozisyonu, gaz besleme debisi gibi parametreler aktiviteyi ve ürün dağılımını etkilemektedir. Tüm bunlara ek olarak katalitik bir reaksiyon olduğu için uygun katalizör geliştirmek büyük önem taşımaktadır.

Bu tez kapsamında hazırlanan katalizörler aktif metal, promotör ve destek malzemesinden oluşmaktadır. Bir aktif metalin destek malzemesi üzerinde homojen dağılması ve başka bir metal ile promote edilmesi istenilen hafif olefin ürün seçiciliğini iyileştirici yönde etkilemektedir. Fischer-Tropsch reaksiyonlarında aktif metal olarak genellikle Fe ve Co tercih edilmektedir. Ulaşımı daha kolay, daha ucuz ve olefin seçiciliği daha yüksek olduğundan bu çalışmada da Fe katalizörü tercih edilmiştir. Destek malzemesi olarak ise geleneksel olarak alümina ve silika bazlı malzemeler kullanılmaktadır. Fakat bu malzemeler demir ile alüminat ve silikat gibi bileşikleri oluşturduğu için daha inert bir destek malzemesine ihtiyaç duyulmuştur. Bu yüzden de son yıllarda, demir ile etkileşimi az olan karbon yapılı malzemelere ilgi artmıştır. Yüksek yüzey alanı ve ucuz olması sebebiyle de bu çalışma için aktif karbon destek malzemesi olarak seçilmiştir.

Bu tez kapsamında promotörlerin aktif karbon destekli demir katalizörü üzerindeki etkileri incelenmiştir. Mn, Zn, K, Na, Cu, S promotörleri kullanılarak aktif karbon destekli demir katalizörünün hafif olefinlere yönelik seçiciliği artırılmaya çalışılmıştır.

Katalizörden, yüksek CO dönüşümü ve düşük CO<sub>2</sub> seçiciliği beklenmektedir. Hidrokarbon ürün dağılımına bakıldığında ise yüksek olefin seçiciliğinin yanında; metan, parafin ve yüksek karbon sayılı ürünlerin seçiciliğinin düşük olması beklenmektedir.

Bu kapsamda toplamda 16 adet katalizör sentezlenmiştir. Demir oranı kütlece %10 olarak belirlenirken, promotörlerin 10Fe üzerindeki farklı kombinasyonları incelenmiştir. Mn, Zn ve Cu promotörleri kütlece %2 ve Na ve K promotörleri kütlece %1 oranlarında eklenmiştir. Na ve S ile promote edilmiş katalizör ise kütlece %0.3 Na ve kütlece %0.1 S içermektedir. *Incipient wetness impregnation* yöntemi ile hazırlanan katalizörler; sıralı ve birlikte impregnasyon yapılarak hazırlanmıştır. Metallerin destek malzemesine iyi bir şekilde dağılımını sağlamak için impregnasyon sırasında toz karıştırma makinesi kullanılmış ve katalizörler ultrasonik banyoda 15 dk bekletilmiştir. Katalizörler sentezleme adımlarından sonra kurutma, kalsinasyon, indirgeme gibi işlemlerden geçerek reaksiyona hazır hale gelirler.

Sentezlenen katalizörlerin fiziksel ve yapısal özelliklerini inceleyebilmek için Scanning Electron Microscope Energy Dispersive X-ray (SEM-EDX), Brunauer–Emmett–Teller (BET), X-Ray Diffraction (XRD), H<sub>2</sub>-Temperature Programmed Reduction (H<sub>2</sub>-TPR) karakterizasyonları yapılmıştır.

Reaksiyon yüksek sıcaklık ve basınçta çalışma imkânı sunan *high throughput screening* sisteminde gerçekleştirilmiştir. Yüksek olefin seçiciliği veren optimum reaksiyon sıcaklığı ve basıncına karar vermek için 10Fe ve 10Fe-2Mn katalizörlerinde 3 farklı reaksiyon koşulu denenmiştir: 260 °C–10 bar; 340 °C–10bar ve 340 °C–20 bar.

Reaksiyon ilk 20 saat 260 °C sıcaklıkta ve 10 bar basınçta yapılmıştır. Daha sonra basınç sabit tutularak sıcaklık artışının etkisine bakmak için sıcaklık 340 °C'ye yükseltilmiştir. Sıcaklık artınca her iki katalizörde de hafif olefin seçiciliğinin arttığı görülmektedir ve Mn eklenmesi de olefin seçiciliğini artırmış fakat aktiviteyi fazla iyileştirmemiştir. Basınç etkisini incelemek için sıcaklık 340 °C'de sabit tutularak basınç 20 bara çıkarılmıştır. Her iki katalizörün dönüşümleri artmış fakat olefin seçicilikleri azalmıştır. Tüm bunlar göz önünde bulundurulduğunda optimum reaksiyon koşulunun 340 °C ve 10 bar olduğuna karar verilmiştir. Ayrıca tüm reaksiyonlar H<sub>2</sub>/CO = 1 ve GHSV = 2000 h<sup>-1</sup> koşullarında gerçekleştirilmiştir.

Aktif karbon destekli demir katalizöründe aynı miktarlarda eklenen sıralı (10Fe-2Mn) ve birlikte (10Fe2Mn) impregne edilmiş Mn promotörü ile yöntem etkisi incelenmiştir. Birlikte impregne edilmiş katalizör daha yüksek olefin verimine sahiptir. Bu da katalizör sentezlenirken bir kalsinasyon adımının atlanması ve daha az ısıl işleme maruz kalması ile ilişkilendirilmiştir. Daha az ısıl işleme maruz kalmış katalizörlerde sinterleşme daha az olmaktadır ve bu da aktif metal kaybını engellemektedir.

10Fe2Mn yanında 10Fe2Zn ve 10Fe-2Cu katalizörleri de promotör etkisini incelemek için sentezlenmişlerdir. Bu üç katalizör içinde en çok O/P oranına 2.0 değeri ile sahip olan 10Fe2Mn; en yüksek dönüşüme sahip olan ise %65 ile 10Fe2Zn katalizörüdür. Cu promotörlü katalizör %25 ile en düşük CO<sub>2</sub> seçiciliğine sahiptir.

Zn, K ve Na promotörleri 10Fe2Mn katalizörü üzerine sıralı impregnasyon ile eklenmiş ve etkileri incelenmiştir. Na ve K promotörü dönüşümün hem artmasına hem de kararlılığa yardımcı olmuşlardır. Promotörlerin eklenmesinin hafif olefin seçiciliğinde büyük bir etkisi olmamıştır. O/P oranı ise en yüksek 10Fe2Mn-1K katalizöründe 4.3 değeri ile başlamış ve 160 saat sonunda 2.4 değerinde kararlılığa ulaşmıştır.



Mn, K ve Na promotörleri 10Fe2Zn katalizörü üzerine sıralı impregnasyonla eklenmiştir. K ve Na eklenmesi dönüşümde negatif etki yaratmamıştır. Mn ise katalizörün aktivitesini en çok düşüren promotördür. Mn, K ve Na eklenen (10Fe2Zn-2Mn, 10Fe2Zn-1K, 10Fe2Zn-1Na) katalizörlerin hafif olefin seçicilikleri birbirlerine yakın olup 10Fe2Zn katalizörünün hafif olefin seçiciliğinden büyüktür. K eklenmesi hem olefin seçiciliğini artırmış ve CH<sub>4</sub> seçiciliğini düşürmüştür. O/P oranında ise 10Fe2Zn-1K katalizörü 5.6 ile yüksek değerde başlamış ve reaksiyon sonunda 2.7 değerine gelmiştir.

Mn, Zn, K ve Na promotörleri sıralı impregnasyon yöntemi ile 10Fe-2Cu katalizörüne eklenmiştir. K ve Na eklenmesi metan seçiciliğini azaltmıştır. Tüm katalizörler arasında en yüksek O/P oranı veren katalizör 10Fe2Cu-1K'dır. 6.3 değeri ile en yükseğe ulaşmıştır ve reaksiyon sonunda 3.8 değerine düşmüştür. Bu düşüşe rağmen en iyi O/P oranını veren katalizör olmuştur.

Na ve S etkisini incelemek için ise 10Fe0.3Na0.1S katalizörü sentezlenmiştir. Fakat olefin seçiciliğinde %20 değerinin üstüne çıkılamamıştır. Bu durumun yüksek sıcaklıkla yapılan testte düşük H<sub>2</sub>/CO oranından kaynaklandığı düşünülmektedir. Bu katalizörle O/P oranı 2.0 elde edilmiştir.

Kendi gruplarında en iyi çıkan katalizörler 10Fe2Mn-1K, 10Fe2Zn-1K 10Fe-2Cu-1K karşılaştırılmıştır. CO dönüşümü en yüksek olan 10Fe2Zn-1K katalizörüdür. Cu içeren katalizörün dönüşümü daha yüksek değerden başlamıştır bu da bakırın, demirin indirgenmesini iyileştirdiğini göstermektedir. 10Fe2Mn-1K katalizörünün olefin seçiciliği %20 civarlarındaiken diğer katalizörlerin olefin seçiciliklerinden daha düşüktür. O/P oranına bakıldığında ise Cu-K kombinasyonu en iyi sonucu vermiş Zn-K onu takip etmiştir.

Tüm bunların yanında katalizörlerin hafif olefin ürün verimleri de hesaplanmıştır. 160 saatlik reaksiyon sonunda 10Fe2Zn-1K katalizörü  $3.4 \times 10^{-3}$  gC/gFe.s ile en yüksek olefin verimine ulaşan katalizördür.

Sonuç olarak, AC destekli 10Fe2Zn-1K ve 10Fe-2Cu-1K katalizörleri endüstriyel kullanım için umut vadetmektedirler.



## 1. INTRODUCTION

Olefins, or alkenes, are the unsaturated hydrocarbon compounds. Ethylene ( $C_2H_4$ ), propylene ( $C_3H_6$ ) and butylene ( $C_4H_8$ ) are called light or lower olefins and shown as  $C_2=C_4$ . Light olefins are key blocks in the chemical industry. Products which are manufactured from light olefins such as plastics, packing materials and solvents are widely used in daily life. Light olefins are also the largest-volume produced chemicals in the world and the demand for those products is increasing day by day, especially for ethylene [1].

Light olefins are produced from crude oil industrially. These chemicals are produced by fluid catalytic cracking of oil or naphtha steam cracking processes. Taking into account the rapid depletion of crude oil reserves, price fluctuations, dependence on foreign sources as well as concern about environment make non-oil based feedstocks more desirable to obtain light olefins. Especially, using syngas ( $CO$  and  $H_2$ ) derived from natural gas, coal, or biomass for the production of light olefins has attracted considerable attention in recent years [2, 3].

Fischer-Tropsch synthesis is the catalytic conversion of syngas into hydrocarbons. The feedstocks of FT are coal, natural gas and biomass. These feedstocks are converted to syngas then hydrocarbon products from methane to  $C_{19+}$  are produced by Fischer-Tropsch synthesis. Regarding the wide range of product distribution of FT, the production of light olefins can be possible. Production of light olefins directly from syngas, is called 'Fischer-Tropsch to Olefins (FTO)'. FTO process needs to be improved for countries with limited oil but large reserves of coal, biomass or natural gas [1, 4]. In this context, syngas can be obtained by gasification of Turkey's lignite which has lower calorific value, thus syngas can be used to produce light olefins.

Parameters such as temperature, pressure, gas composition and flow rate affect activity and product distribution of FTO reaction. Catalyst plays very important role for FTO. The catalyst is expected to have high  $CO$  conversion, high selectivity to light olefins and low selectivity to  $CO_2$ ,  $CH_4$ ,  $C_2-C_4$  paraffin and  $C_{5+}$  products.

In literature, a wide variety of catalysts have been investigated for selective light olefins production with different active metals, promoters and support materials. However, researchers have encountered several problems such as lower catalytic activity, deactivation of the catalyst in a short time, coke formation, and high carbon number products.

Catalysts prepared in this thesis consist of active metal, promoter and support material. Support material enhances the active metal dispersion and product distribution can be shifted to desired products in the presence of promoter. Iron (Fe) was preferred as an active metal in this study since it is abundant, inexpensive and has higher olefin selectivity. Conventionally,  $\text{Al}_2\text{O}_3$  and  $\text{SiO}_2$  supports are used for catalyst synthesis for FTO but they have a strong interaction with Fe, resulting in Fe-Al or Fe-Si [5]. Recently, carbonaceous materials (activated carbon, carbon nanotube (CNT), ordered mesoporous carbon (CMK-3), graphene oxide (GO)) have attracted attention because they have a high surface area that allows the higher dispersion of active metal on a support. Activated carbon was chosen as the support material for this study with regard to its high surface area and low cost [6].

Different metals have been investigated as promoters to improve the light olefins selectivity such as Mn, Zn, K, Na [7–12]. Asami et al. [13] and Tian et al. [14] suggested that Mn promoter suppresses the hydrogenation of olefins. Ribeiro et al. [11] suggested that adding alkali promoters decrease the C–O bond strength. An et al. [12] and Cheng et al. [15] found that K enhances the surface basicity and it facilitates the electron-donation between Fe and CO. Galvis et al. [16] studied Na and S promoters on  $\text{Al}_2\text{O}_3$  and achieved the ~50% selectivity to light olefins. Oschatz et al. [17] synthesized catalyst of Fe, Na and S over carbon black support and light olefins selectivity was found 58%. Zn promoted Fe catalyst was tested by Gao et al. [9] and they found that the Zn promoted catalyst show better performance and catalytic activity. Schulz et al. [18] worked on Cu promoter and found out that Cu facilitates the Fe reduction.

In this study, I investigated the effect of Mn, Zn, Cu, K, Na and S promoters over the AC supported Fe catalyst by screening with high throughput test system. Different combinations and amounts of promoters were loaded to obtain the high selectivity to light olefins.

## **1.1 Purpose of the Thesis**

The main purpose of the thesis was to synthesize promoted and supported catalysts which have high selectivity to light olefins in Fischer-Tropsch synthesis. To achieve this aim; AC is used as a support material and Fe which has high activity for FT is used as an active metal. Mn, Zn, Cu, K, Na and S promoters were separately or in groups added to catalyst to improve the FTO activity and light olefins selectivity. Besides improving activity and light olefins selectivity, lowering the selectivity toward undesired products such as CO<sub>2</sub>, methane, paraffin and higher hydrocarbons were aimed.

## **1.2 Thesis Plan**

Chapter two includes a literature review about light olefins in the chemical industry, detailed information of Fischer-Tropsch reaction and catalyst design considerations of Fischer-Tropsch to olefin process. Catalysts preparation procedure and performance tests of catalysts are explained in detail in Chapter 3. Catalyst performance test results are presented and discussed in Chapter 4. Chapter 5 includes the conclusion of the current study.



## 2. LITERATURE REVIEW

### 2.1 Light Olefins in Chemical Industry

Ethylene ( $C_2H_4$ ) is one of the petrochemicals produced in largest volume worldwide since it is the raw material of a wide of range chemicals such as plastics, fibers, and other organic chemicals. Ethylene is used as a monomer to produce polyethylene, PVC, polystyrene, polyether's polyesters. It is also used in the production of intermediate chemicals such as ethylbenzene, ethylene oxide and ethylene dichloride which have high importance in the industry. These ethylene derived chemicals are the feedstock of the packaging, construction and textile products. 62% of total ethylene is consumed to produce polyethylene. The next-largest volume derived is ethylene oxide and it is used to produce ethylene glycol (EG), which is used primarily in the manufacturing of PET.

Most of the ethylene produced by naphtha cracking in Europe and Asia however in U.S. and Middle East ethylene is produced by ethane and propane cracking [1]. Figure 2.1 shows the ethylene production in metric tons in the United States and Western Europe, including Norway. Western Europe involves ethylene production in Turkey in 2015 and 2016 [19–22]. In 2018, the U.S. production volume of ethylene amounted to a total of approximately 30 million metric tons.

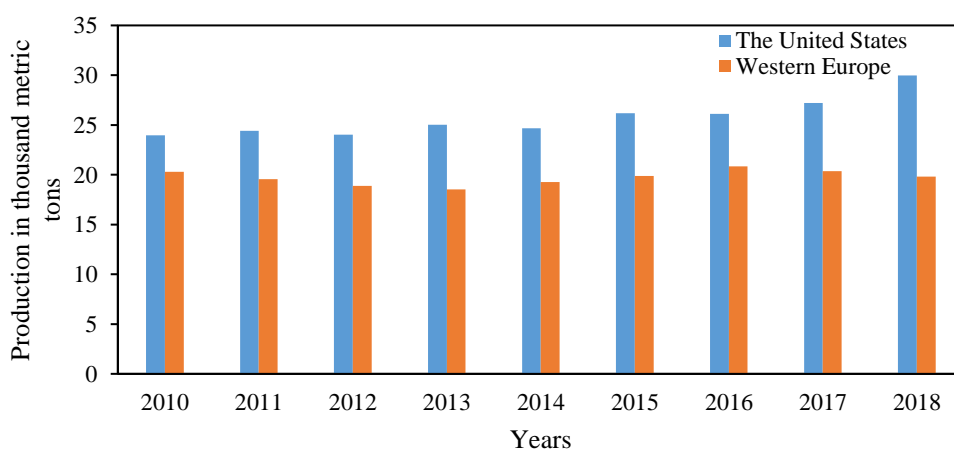


**Figure 2.1** : Ethylene production in the United States and Western Europe between 2010 and 2018 [19, 21].

Propylene ( $C_3H_6$ ) is a chemical which has the second largest production volume after the ethylene. Propylene is the raw material for the production of organic compounds. Propylene is used production of polypropylene, propylene oxide acrylics, urethanes, phenolic resins and polymethyl methacrylate (PMMA). In 2016, about 65% of produced propylene is used in the manufacture of polypropylene resins. About 8% of the world's propylene is used in the production of propylene oxide which is a precursor of the propylene glycol and polyols. The propylene production in metric tons in the United States and Western Europe, including Norway, are shown in Figure 2.2. Also, propylene production in Turkey is included within Western Europe in 2015 and 2016 [19, 22–24]. In 2018, the U.S. production volume of propylene amounted to a total of 16 million metric tons.

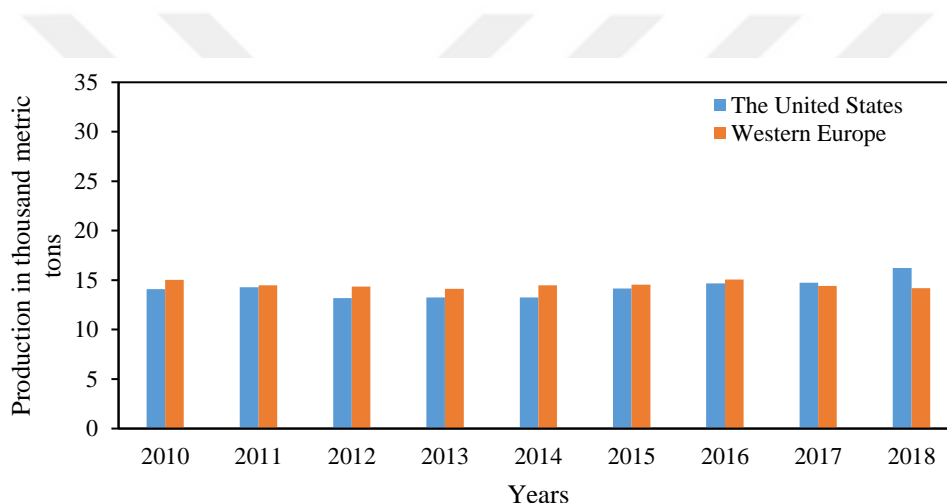


**Figure 2.2 :** Propylene production in the United States and Western Europe between 2010 and 2018 [19, 24].

Butylene ( $C_4H_8$ ), also known as butene, consists of a series of alkenes (isomers) that have four carbon atoms. The isomers are butadiene, isobutylene, and n-butene. The  $C_4$  olefins play a very important role in fuel and chemical materials production. Polybutadiene, nylon 6,6 and styrene-butadiene rubber (SBR) are the derivatives of butadiene [19].

## 2.2 Light Olefin Production Using Syngas

There are several alternative processes for the production of light olefins which are listed below.



- Dehydrogenation of lower paraffin,
- Syngas based processes
- Special processes for desired products as ethylene via ethanol dehydration process which obtained from renewable sources or propylene production via propane dehydration which is a byproduct of biodiesel.

Focusing on syngas derived from coal or biomass, there are several process routes to obtain light olefins as it is seen in Figure 2.3.

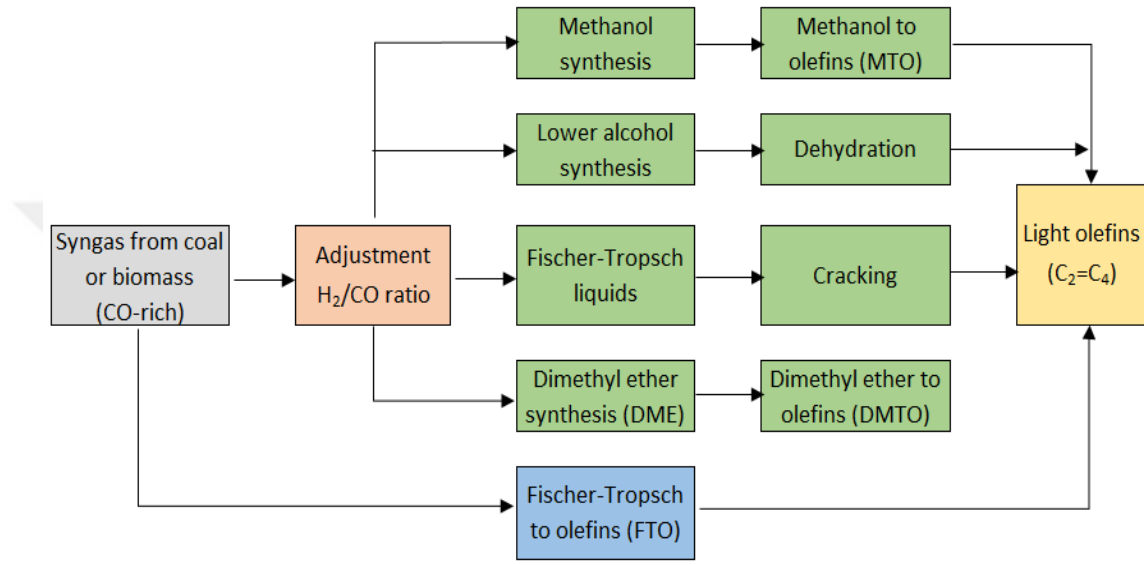


**Figure 2.3 :** Indirect (green) and direct (blue) processes for the production of light olefins [1].

These process routes can be divided into two parts: indirect processes that have intermediate products such as methanol, alcohol, etc. and the other one is direct processes which can be possible via FT synthesis and called as ‘‘Fischer-Tropsch to Olefins (FTO)’’ [1].

### 2.2.1 Indirect processes

Some indirect processes have been developed for light olefins production. Indirect processes can be seen in Figure 2.3. Methanol to olefins (MTO) process has been developed where the MTO technology over the steam cracking and natural gas conversion economically. MTO processes have been generally investigated on zeolite support like SAPO-34. The main product of MTO is ethylene when the SAPO-34 support is used. Up to 90% of light olefins are obtained from methanol but the catalyst

activity decreases rapidly by the coke formation depending on the crystal size of catalyst and the reaction conditions [25].

Dimethyl ether to olefins (DMTO) is another indirect process. The dimethyl ether synthesis from syngas is thermodynamically more favorable rather than the methanol formation. The process consists of two reactions; in the first reactor, DME production is carried out with a bifunctional catalyst, and the second reactor light olefins obtained with a SAPO-34 catalyst. Dong et al. [26] developed the Cu-Zn/ZSM-5 catalyst for DME formation from syngas then to get the high selectivity 90 wt.% towards to light olefins using by metal modified SAPO-34 catalyst.

### **2.2.2 Direct processes**

Direct process means to obtain light olefins without an intermediate product. Fischer-Tropsch synthesis, as it leads to direct conversion of CO to hydrocarbon, is a good opportunity compared to indirect processes like MTO, DMTO and cracking of FT liquids. FTO reaction has got attention for more than 50 years and many researchers have studied different catalysts to obtain light olefins. # of publications on FTO, increased with increasing oil price [27, 28].

After the oil embargo of 1973 and the oil crisis in 1979, number of patents for the direct synthesis of light olefins from syngas hit the maximum number. The high price of the oil led to a search of alternative processes to obtain light olefins instead of the naphtha cracking. Oil prices increased sharply after the Invasion of Iraq in 2003. The rise in the oil price caused the search of alternative processes to produce light olefin from syngas again. In 2010, oil prices increased again because of the political instability in the Middle East [1].

## **2.3 Fischer-Tropsch to Olefins**

### **2.3.1 Fischer-Tropsch synthesis**

With the rapid development and growth of the transport industry in the 1920s, countries with limited access to crude oil but had coal reserves begun to search alternative processes for the production of fuels. Two scientists, Franz Fischer and Hans Tropsch invented a process to convert coal into liquid hydrocarbons at the Kaiser Wilhelm Institute for Coal Research (KWI) in Mulheim Ruhr, in 1926 [2].

Fischer and Tropsch produced syngas by steam hydrocracking of coal then syngas was converted to synthetic liquid when operation conditions were in the range of 1 to 10 atm. and 180 to 200 °C. The cobalt-based catalyst was first used and developed by Fischer and Tropsch. The aim of the process was to obtain liquid fuels from coal or another carbon source that is not oil-based. Until the end of the 20<sup>th</sup> century, Germany exported the FT technology to the USA, Britain, South Africa, Japan and France [29]. In 1936, FT technology was industrialized and commercialized by Ruhrchemie AG. The industrial capacity of FT plant was almost 600 thousand tons per year in Germany. After World War 2, FT process developments gained prominence because of the rapid increase of fuel consumption and limited petroleum sources.

The first FT plant in South Africa, Sasol 1, was built up in 1952. Because of the energy crises in the 1970s, crude oil prices increased. Two more FT plants were established by Sasol until the 1990s [2].

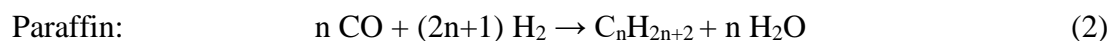
Raw material of Fischer-Tropsch synthesis is synthetic gas or syngas. Syngas mainly consists of CO and H<sub>2</sub>. The feedstock of syngas could be coal, natural gas or biomass. FT processes are named based on the used feedstock hence the terminology is ‘coal to liquids’ (CTL), ‘gas to liquids’ (GTL) and biomass to liquids (BTL) [4].

Although, FT process is used to produce liquid hydrocarbons, this study is focused on producing gaseous light olefins via Fischer-Tropsch synthesis (FTO). Reaction proceeds in the same way but the production should be oriented towards getting higher light olefins selectivity. This can be possible with catalyst and reaction conditions that give high conversion and olefin selectivity.

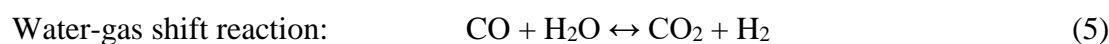
Chemical processes that take place in Fischer-Tropsch synthesis can be expressed by the following general reaction equation:



Although the FT reaction is described by a single reaction equation, a large number of reactions occur in the reactor during the process, resulting in a wide variety of hydrocarbon products. These products are paraffins, olefins and some amount of oxygenates. The main parameters affecting the product distribution are operation temperature and pressure, feed gas composition and the catalyst. The following exothermic reactions take place during FT synthesis [30].



In addition these main hydrocarbon productive reactions, there are side reactions that during Fischer-Tropsch synthesis: Water-gas shift (WGS) and Boudouard reaction [30].



FT process is divided into 2 parts according to operation conditions:

1. High-temperature FT (HTFT)
2. Low-temperature FT (LTFT)

The operating temperatures of HTFT and LTFT are between 300-350 °C and 200-240 °C respectively. As the fuel products obtained from Fischer-Tropsch synthesis at LTFT conditions efficiently, HTFT conditions are more appropriate for the production of valuable chemicals [31]. Since the aim of this study is producing light olefins high temperature is required.

### 2.3.2 Fischer-Tropsch mechanism and product distribution

Fischer-Tropsch mechanism has attracted many researchers. Reaction starts with hydrogenation of CO followed by C-C bond formation then leading to chain growth which makes the FT be considered as a polymerization reaction. Studies about the mechanism are still ongoing however the surface carbide mechanism is the most accepted mechanism [1, 29].

Adsorption of CO on the catalyst surface leads to the reaction in the carbide mechanism. The metal surface is carbided by the carbon that comes from dissociative adsorption of carbon monoxide. The second reactant hydrogen is also dissociatively adsorbed on the active metal. CO is adsorbed on active metal stronger than hydrogen [29].

The FT reaction proceeds following these steps:

1. reactant adsorption;
2. chain initiation;
3. chain growth;
4. chain termination;

5. product desorption;
6. readsorption and further reaction.

The carbide mechanism is given in Figure 2.4. In the first step, the reactants are adsorbed on the metal surface. The second step is the chain initiation when the C hydrogenation begins. In the third step, C addition occurs which called as chain growth. In the fourth step, the chain terminates to form olefins and paraffins. Product desorption follows these steps and reactants are adsorbed again the same procedure occurs [32].

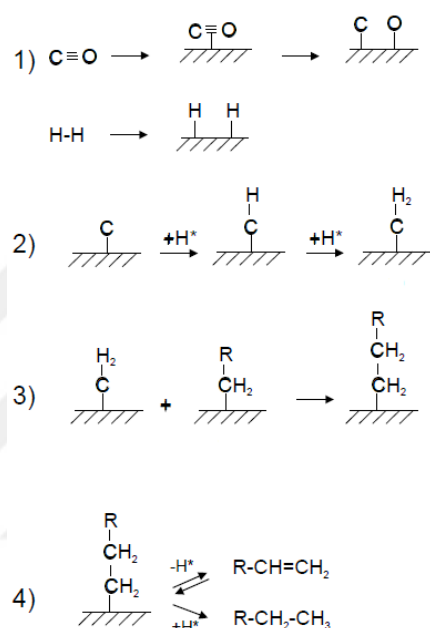


**Figure 2.4 :** The mechanism of Fischer-Tropsch reaction [32].

As it is seen in Figure 2.5, product distribution is so wide and needs some parameters to predict the C atom numbers of hydrocarbons. Anderson-Schulz-Flory (ASF) model predicts the product distribution of Fischer-Tropsch reaction with a chain growth probability ‘ $\alpha$ ’. The chain growth probability depends on the promoters, reaction conditions, catalyst type, etc. [1].

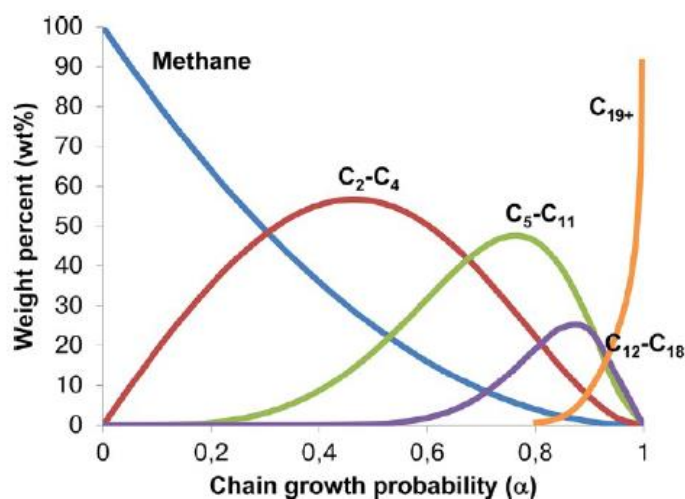


**Figure 2.5 :** Anderson-Schulz-Flory (ASF) model [1].

Considering the maximum C<sub>2</sub>=C<sub>4</sub> light olefins selectivity via FTO, the alpha value is between 0.4 and 0.5 according to the ASF model. The reaction temperature has an influence on the alpha value. The alpha value can be lowered by rising the reaction temperature. Methane selectivity gets higher with a low chain growth probability value however, methanation is not the desired reaction for FTO. That is why the direct conversion of syngas to light olefins via FT is cannot be applied to industrial scale [27, 28].

It should be noted that the ASF model is important as an approach, but that there may be deviations (negative-positive) from the model. Negative behavior about the high methane selectivity is observed on the Fe-based catalyst. Fe has different structures during the reaction, some of them responsible for the chain growth while others responsible for the methane formation. These different Fe structures can be modified adding some promoters. Torres Galvis et al. [16] achieved low methane selectivity as well as the high selectivity towards light olefins adding Na and S promoters to Fe catalyst. Na and S promotion provides the selective blockage of hydrogenation sites. Thus, adding promoters can change the product distribution.

There is an enormous amount of research studies about the different aspects of the FT synthesis such as reaction mechanisms, industrial application, and FT catalysts that are discussed in various review articles and books [4, 31, 33].

Specific studies related to the catalyst preparation methods, application, and deactivation of Fe as the catalysts active phase used in the FT process for liquid fuel production have been conducted by researchers.

Due to this variety of studies in traditional FT synthesis, this study does not include the general aspects of the FT synthesis and its traditional catalysts. As the purpose of this study, we will further concentrate on designing suitable catalysts for light olefins production via FT process.

## **2.4 Fischer-Tropsch to Olefins Catalysts**

Catalyst plays a very important role in FT the reactions.

Catalyst selection considerations:

- Cost
- Easy availability
- Desired product selectivity
- Stability
- Activity

Activity and product distribution mainly depend on the structure of the catalyst. Considerations of catalyst design are chemical, mechanical, and physical properties of the catalyst. Size of the catalyst and active metal orientation are also other factors that must be considered [4].

High catalytic activity, high selectivity towards light olefin, low methane, paraffin, C<sub>5+</sub> selectivity and low CO<sub>2</sub> selectivity are expected from the FTO catalyst.

### **2.4.1 Active metal**

Reaction proceeds on active metal sites. It provides the active phase formation. For the application of FT; Fe, Ni, Co and Ru metals show activity. As a price comparison, taking the Fe reference as 1.0, the approximate price of Ni is 250, of Co is 1000 and of Ru is 50.000. Ni-based catalysts have high selectivity toward CH<sub>4</sub>. Ru is the most expensive active metal and it is not abundant. That high price makes it not appropriate for industrial-scale applications. As a result, there are two viable metals; Fe and Co [31].

Regarding the product spectrum, Fe produces more olefins and oxygenates than cobalt which may be related to lower hydrogenation affinity of Fe. When Fe is used it changes its form to carbide or oxide during the FT but Co is active in the metallic state [4].

For Fe catalyst, at lower temperatures (220–250 °C) the chain growth probability ( $\alpha$ ) is approximately 0.94 indicating that the catalyst can produce higher carbon numbers (longer than C<sub>21</sub>) compounds. In the other case, when the temperature is higher (320–350 °C) the chain growth probability ( $\alpha$ ) decreases to 0.7 and even lower. The lower ( $\alpha$ ) value gives a chance to produce transportation fuels and valuable chemical feedstocks, for example, light olefins [4].

As it is described before Fe is more suitable choice as the active metal for FTO with high olefin selectivity, high activity. Unfortunately, Fe catalyst deactivation is more quickly in comparison to the Co-based catalysts [34].

#### 2.4.2 Promoters

To enhance the performance of the catalysts promoters are added to the catalysts during the preparation. Promoters affect the structural properties of the catalysts by changing the electronic character of the metallic active phase which results in improved activity and selectivity of the catalysts. Different kinds of metals such as alkali metals (Na, K) and transition metals (Mn, Zn, Cu, and Pt) are generally used as promoters in Fe or Co-based catalysts designed for FT synthesis [30].

Li et al. [35] studied the effect of Mn on the activity of the Fe catalyst on light olefin production. Catalysts containing different Fe/Mn atomic ratio of 100/x (x= 0, 3, 7, 12, and 23) were synthesized by using the combination of both spray drying and co-precipitation methods. The samples were tested under the reaction conditions of 1.5 MPa, H<sub>2</sub>/CO= 2, and a temperature of 250 °C. It was observed that the sample containing Fe/Mn= 100/7 exhibited better activity than the other samples and light olefin to light paraffin ratio of 3.17. Surface basicity was improved with Mn incorporation and that led to obtaining high olefin selectivity.

In another study conducted by Tian et al. [14] the effect of KMnO<sub>4</sub> on the AC supported Fe-based catalyst activity in the FT synthesis was investigated. Four samples treated 0, 0.02, 0.05, and 0.1 M KMnO<sub>4</sub> which were coded as Fe-AC, Fe-2MnK-AC, Fe-5MnK-AC, and Fe-10MnK-AC were synthesized by incipient wetness impregnation method. As a result of KMnO<sub>4</sub> treatment, CO adsorbed more on catalyst. The catalyst was reduced *in-situ* at 300 °C for 12 hours and they were tested at 320 °C, 2 MPa, and H<sub>2</sub>/CO= 1. It is reported that the sample named Fe-2MnK-AC has shown CO conversion c.a. 96% and 27% selectivity to light olefins.



To study effects of the K promoter on Fe catalysts supported on reduced graphene oxide (rGO). Cheng et al. [15] prepared four catalysts including FeK0.5/rGO, FeK1/rGO, FeK1.5/rGO, and FeK2/rGO, in which the numbers stand for K contents of 0.5% - 2%. Catalysts prepared by using impregnation method. Samples were reduced under 5% vol. H<sub>2</sub>/Ar flow at 723 K for 16 h. The reaction took place at 613 K and 20 bar with syngas ratio of H<sub>2</sub>/CO/N<sub>2</sub> of 48/48/4. It has been shown that K promoter had no effect on CO conversion, it affected the light olefins selectivity which was increased from 31% in the unpromoted catalyst to 68% in the FeK2/rGO sample. The best iron time yield (FTY) for olefin products was achieved by FeK1/rGO. To study the basicity of K, CO<sub>2</sub>-TPD was used to determine the basicity effect of K on the catalyst surface. Adsorbed CO<sub>2</sub> increased with an increase in K content. So, this characterization affirms that K helps to enhance the basic sites on the catalyst surface. According to CO-TPD profile, adsorbed CO increased; indicating that in the presence of K the interaction between Fe and CO is improved by facilitation electron-donation from the iron to CO. Also, K promoter has suppressed the paraffin and methane production. Also,  $\chi$ -Fe<sub>5</sub>C<sub>2</sub> was identified as an active phase for FTO.

Ma et al. [36] studied the effect of K on the activity and product distribution on AC supported Fe catalysts. 15.7% Fe/AC, 15.7% Fe/0.9 K/AC and 5.7% Fe/2K/AC catalyst were synthesized to investigate K effect on catalyst. Catalytic activity increased when the 0.9 wt.% K was added compare to 2 wt.% K. 0.9 wt.% K catalyst showed the significantly higher olefin/paraffin ratio than the unpromoted and 2 wt.% K catalyst as well. Also, K promoter suppressed the methane formation. Also, K promoter enhanced the electron density on Fe and made the Fe-C bond stronger

Several studies have investigated effects of alkali metals on supported iron-based catalysts in FT synthesis. To study these effects Xiong et al. [37] prepared carbon nanotubes (CNTs) supported iron catalyst containing 10 wt.% iron. These catalysts were promoted by Li, Na, and K with a Fe/alkali metal ratio of 100:3.4. H<sub>2</sub> temperature-programmed reduction (TPR) experiment showed that Li promoter improved the reduction by decreasing the reduction temperature. Conversely, Na and K promoters inhibited the reduction of K. K and Na promoted catalysts enhanced the light olefins selectivity, suppressed methane and shifted products towards higher molecular weight hydrocarbons. In addition, they found that K promotion lowered the catalytic activity whereas Na increased it.

In a recent study, Zhao et al. [38] investigated the effects of Zn, Al, Ti, and Si as promoters on the Fe catalysts. Samples with the promoters were synthesized by co-precipitation method. The reaction condition in which samples were tested was  $T = 350$  °C, 2 MPa, and  $H_2/CO = 2.7$ . At the end of the 12 h reaction test, Zn promoted catalyst exhibited a higher CO conversion of around 95% and the light olefin yield of 43% which was the highest values compared to other promoted samples.

Asami et al. [13] synthesized Fe-Cu/AC catalyst with a weight ratio of Fe/Cu/AC:100/1/100 employing co-precipitation method.  $H_2/CO = 1$ , 300 °C and 2.0 MPa were the reaction conditions for FTO. Mn and K promoters were added to Fe-Cu/AC which had 41 wt.% Fe. The addition ratio of metal/Fe was 0.3. In the increase of light olefins was observed on Mn. When Mn was loaded the selectivity of lower olefins increased from 25% to 33% and olefin/paraffin ratio from 2.1 to 4.5. This implicates that manganese introduction should suppress the further hydrogenation of olefins. Then they tried the Mn/Fe ratio 0.1, 0.3 and 0.5 to investigate how Mn amount effects the FTO. The catalytic activity tended to decrease with increasing Mn amount. On the other hand, with an increase in Mn composition first olefin selectivity increased until 0.3 then it decreased.

In some cases, Na and S have been used as promoters for Fe catalysts. Although, high quantities of sulfur can poison the catalyst resulting in its deactivation, small amounts of it as a promoter have shown positive effects on the light olefins selectivity. To study the effects of Na and S promoters on the  $\alpha$ - $Al_2O_3$  supported iron catalysts, Galvis et al. [16] loaded 0.2 wt.% Na and 0.03 wt.% S on 5 wt.% Fe catalysts, separately. After a 20 h reaction at 340 °C, 20 bar, and  $H_2/CO = 1$  it was reported that the addition of 0.03% S decreased methane selectivity from 27% to 16%. On the other hand, light olefins selectivity increased by 17% (from 35% to 41%). Na promoter did not significantly affect CO conversion in that research study and it has reduced both the light olefins selectivity and methane selectivity of the catalyst.

Oschatz et al. [17] Na and S promoter content on iron (10 wt.%) catalyst supported carbon material. The reaction proceeds at  $H_2/CO = 2$ , temperature and pressure were 340 °C, 10 bar respectively. Na promoter was loaded between 1-30 wt.% whereas S was loaded between 0.5-5 wt.% with respect to Fe. They reported that low Na loading (1-3 wt.%) led to inhibition of forming of Fe to Fe carbide. High Na contents, (15-30

wt.%) causes the particle growth because of the Na covers the Fe particles during FTO operation. The optimum loadings were reported as 1-3 wt.% Na and 0.5-1 wt.% S with respect to iron due to the high activity and slower decrease in activity. To decrease the methane and C<sub>2</sub>-C<sub>4</sub> paraffin selectivity a small amount of alkali was required. The effect of the S was blocking the hydrogenation sides of the iron.

Schulz et al. [18] reported that copper enhanced the reduction of iron. After that investigation, Ma et al. [39] studied 0-2 wt.% copper addition on 15.7 wt.% Fe and K content 0.9 wt.%. Adding 0.8-2 wt.% copper improved the reduction temperature of the catalyst according to TPR profiles. Also, Cu promoted the hydrogen adsorption on the catalyst surface. The catalytic activity of Fe-K/AC decreased with increased Cu content.

To summarize the effect of promoters Table 2.1 was prepared.

**Table 2.1** : Promoters used in Fe based catalysts and their effects.

Promoters	Effect of promoter
Mn	- Suppress the hydrogenation of olefins - Stabilize the activity
Zn	- Better CO conversion and stability
Cu	- Facilitates reduction of iron oxides to metallic iron - Enhances the reduction temperature
K	- Enhances surface basicity, it has a strong effect on adsorption of reactants on the active metal - Lower selectivity to methane and paraffin
Na	- Chain growth probability and C <sub>5+</sub> selectivity decreases at lower sodium content
S	- Blocks the hydrogenation sides of the iron - Suppresses methane and paraffin formation

### 2.4.3 Unsupported Fe catalyst

Unsupported Fe catalysts have been investigated high selectivity towards light olefins. Bulk Fe catalysts exhibited high selectivity towards light olefins by the addition of promoters [40]. When the reaction operates at high temperature, bulk iron catalysts are mechanically unstable. Sintering of the particles hinders the adsorption of the reactant on the active metal and carbon deposition occurs which can block the active phase [8].

### 2.4.4 Supported Fe catalyst

Although some catalytic materials are made from a single material, catalysts may consist of three components as it is seen in Figure 2.6:

1. Active metal
2. Promotor
3. Support

Active metal is the most important component of the catalyst. Support and promoter can affect the catalyst surface morphology, distribution, product selectivity, surface area and catalytic performance.

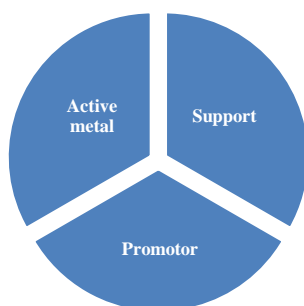


**Figure 2.6 :** Three components of a catalyst.

Support materials are used for maximizing the surface area of the active metal in catalysts. Materials which have a large surface area facilitates better metal dispersion. High dispersion of the active metal may prevent mechanical degradation which threatens bulk Fe catalysts. For texture properties (pore size, pore structure, specific surface area) of support affects the reduction of active metal and the dispersion of active metal [6].

Traditionally, silica ( $\text{SiO}_2$ ) and alumina ( $\text{Al}_2\text{O}_3$ ) have been studied as support material. Recently, carbonaceous materials (AC, CNT, CMK-3, GO) have attracted attention because having a high surface area which allows for a higher dispersion and smaller particle size of the active metal [6]. Modification ability and weak interaction with metal oxides make the carbon materials preferred. Weak interaction with metal oxides results in a facile reduction and formation of iron carbides [14].

Silica and carbon support materials were studied by Cheng et al. [5] SBA-15,  $\text{SiO}_2$ , activated carbon, CNT and CMK-3. Supports were loaded with a nominal 10 wt.% Fe by IWI. One of CMK-3 catalyst was prepared with ethanol and it was named as Fe/CMK-3S. BET areas were  $\text{Fe/CMK-3S} > \text{Fe/SBA-15} > \text{Fe/AC} > \text{Fe/SiO}_2 > \text{Fe/CNT}$ . Besides the different textural properties and morphologies, carbonaceous materials have surface functional groups like hydroxyl, carboxyl. Calcined silica catalysts contained hematite ( $\text{Fe}_2\text{O}_3$ ) whereas calcined carbon-based catalysts contained magnetite ( $\text{Fe}_3\text{O}_4$ ) phase as a major Fe phase. That formation of the magnetite phase on carbon supports associated with the partial reduction of Fe during the nitrate decomposition. Partial oxidation of the carbon support by released oxygen during the nitrate decomposition helped the partial reduction of Fe to  $\text{Fe}_3\text{O}_4$  instead of keeping it at the  $\text{Fe}_2\text{O}_3$  phase. To confirm the partial oxidation of carbon support, unloaded CMK-3 and iron nitrate loaded CMK-3 were heated in He flow to detect  $\text{CO}_2$ . A broad  $\text{CO}_2$  peak was observed for the sample which Fe loaded. Catalyst activation in CO at 350 °C helped the formation of  $\chi\text{-Fe}_2\text{C}_5$ . Catalysts tested at 20 bar, 300 °C and  $\text{H}_2/\text{CO} = 2$ . Fe/AC and Fe/CNT have the highest activities with 64% and 85.4% respectively. The O/P ratio of the  $\text{C}_2\text{-C}_4$  of the Fe/AC is 1.2 and Fe/CNT is 1.4. Methane selectivity values of these two catalysts are the lowest ones.

Cheng et al. [41] studied the support effect for  $\text{SiO}_2$ ,  $\text{Al}_2\text{O}_3$ , CNT and CMK-3 on the iron-based catalyst and even they went a step further by attempting the Na promoter effect. 10 wt.% iron was loaded and catalysts named Fe/Support(x); support indicates the  $\text{SiO}_2$ ,  $\text{Al}_2\text{O}_3$ , CNT and CMK-3 and x refers to the loading of molar ratio Na divided by iron (Na/Fe). The reaction proceeded at 2 MPa, 300 °C with a ratio  $\text{H}_2/\text{CO} = 2$ . Catalyst were sort by the BET areas as  $\text{Fe/CMK-3} > \text{Fe/SiO}_2 > \text{Fe/Al}_2\text{O}_3 > \text{Fe/CNT}$ . FTIR spectroscopy was used to find the possible interactions of active metal Fe and promoter Na with  $\text{Al}_2\text{O}_3$  and  $\text{SiO}_2$  supports. Sodium silicates were detected on spectra which could form strong interaction of  $\text{SiO}_2$  and Na. For  $\text{Al}_2\text{O}_3$ , new broadband

appears which could be assigned to existing carbonates. This result could be because of the interaction of Fe and  $\text{Al}_2\text{O}_3$  to form aluminates that have a strong ability to capture  $\text{CO}_2$ . The presence of sodium generated a new band, it was grounded in the formation of sodium carbonates. In addition to sodium carbonates, sodium aluminates observed in XRD peaks. Between the unpromoted catalysts, Fe/CNT has the highest catalytic activity that might be attributed to placed iron particles in the CNT channels which caused forming the different carbide forms. But increased Na content caused the activity lose for carbon support materials. Fe/ $\text{SiO}_2$  has the lowest activity among the all unpromoted catalysts. The highest olefin/paraffin ratio for light olefins (6.9) and the highest light olefin selectivity (24.1%) achieved with Fe/CMK-3 (0.5). Alumina supported catalysts have low O/P ratio comparing to silica and carbon supported catalysts.

Asami et al. [13] investigated the Cu, Mn, K promoters on AC supported Fe catalysts. Fe and Cu sulfates were used for employing the co-precipitation with a composition Fe/Cu/AC = 100:1:100 by weight. Mn was introduced by co-precipitation with sulfates simultaneously. K was added by incipient wetness impregnation. Fe loading was 41 wt.% and the metal/Fe ratio was 0.3. Reaction conditions were 300 °C, 2 MPa-G and  $\text{H}_2/\text{CO} = 1$ . A possible mechanism of the Fe-Cu/AC catalyst was explained. First,  $\text{H}_2$  and CO adsorbed on the Fe surface dissociatively, then hydrogen species come from the Cu surface. Free  $\text{H}_2$  molecules combine with surface O to form  $\text{H}_2\text{O}$  and  $\text{H}_2\text{O}$  molecules are desorbed. But some of  $\text{H}_2\text{O}$  readsorbed and its oxygen group react with nondissociated CO further  $\text{CO}_2$  is obtained. This reaction is known as the water-gas shift. Carbon species (carbide) hydrogenated to form  $\text{CH}_2$ - and  $\text{CH}_3$ - groups. Alkyl groups ( $\text{C}_n\text{H}_{2n+1}$ ) produced by  $\text{CH}_2$ - insertion that is known as chain propagation. Hydrogenation of alkyl groups ends up with the paraffin products, the  $\beta$ -elimination of alkyl groups leads to form olefins. Also, olefin products could be adsorbed and hydrogenated to form paraffin.

Oschatz et al. [42] were studied the calcination temperature of sodium and potassium promoted iron based catalyst supported over CMK-3 catalyst. The calcination proceeded at 300, 500, 800 and 1000 °C. They found that the particle growth was observed at 800 and 1000 °C and graphitic shell blocking the active sides. To prevent particle growth and graphitic layers calcination temperature can be kept at 500 °C or lower. Specific surface area, pore volume and average pore size increased from 300 to

800 °C which indicates the encapsulation of iron particles is better at lower calcination temperature. The confinement was that the iron particles fill the pores of the support. Blocked pores were not available for the nitrogen. Carbonous materials are partially consumed at high calcination temperatures since carbon tends to oxidation where the oxygen comes from the iron oxide.







### 3. EXPERIMENTAL

#### 3.1 Materials

In this part, materials that were used to synthesize the catalysts are given. Also, properties of these materials can be found.

##### 3.1.1 Chemical materials

Chemicals that are used for catalyst synthesis are listed in Table 3.1.

**Table 3.1** : Chemicals that are used for catalyst synthesis.

Chemicals	Formula	Specification (%)	Supplier
Activated Carbon	AC	Steam activated, acid washed	Alfa Aesar
Iron(iii) nitrate nonahydrate	$\text{Fe}(\text{NO}_3)_3 \cdot 9\text{H}_2\text{O}$	98.0-101.0	Alfa Aesar
Manganese(ii) nitrate hexahydrate	$\text{Mn}(\text{NO}_3)_2 \cdot 6\text{H}_2\text{O}$	98<	Alfa Aesar
Zinc nitrate hexahydrate	$\text{Zn}(\text{NO}_3)_2 \cdot 6\text{H}_2\text{O}$	99.998	Alfa Aesar
Potassium nitrate	$\text{KNO}_3$	99	Alfa Aesar
tri-Sodium citrate dihydrate	$\text{C}_6\text{H}_5\text{Na}_3\text{O}_7 \cdot 2\text{H}_2\text{O}$	99.9	VWR Chemicals
Copper(ii) nitrate hemi(pentahydrate)	$\text{Cu}(\text{NO}_3)_2 \cdot 2.5\text{H}_2\text{O}$	98	Sigma-Aldrich
Iron(ii) sulfate heptahydrate	$\text{FeSO}_4 \cdot 7\text{H}_2\text{O}$	99.5-102.0	Merck

##### 3.1.2 Gases and liquids

Specifications of the liquids and gases used in the experiments are listed in Table 3.2 and Table 3.3, respectively.

**Table 3.2** : Specification of liquids used.

Liquid	Specification	Application
Water	Deionized	Aqueous solutions

**Table 3.3:** Specifications and applications of gases used.

Gas/standard	Formula	Specification	Source	Application
Helium	He	99.99%	Linde	Inert, GC Carrier Gas
Carbon monoxide	CO	95%	Linde	Reactant
Hydrogen	H <sub>2</sub>	99.995%	Linde	Reactant
Nitrogen	N <sub>2</sub>	99.999%	Linde	Inert, Balance

### 3.2 Catalyst Synthesis

Catalysts were prepared by incipient wetness impregnation (IWI) method based on the principle of dissolving salt in the deionized water of organic solution to fill the pore volume of the support material. Activated carbon (Carbon powder, activated Norit GSX, steam activated, acid washed, Alfa Aesar) was used as a support material. Activated carbon was calcined at 300°C for 3 hours under N<sub>2</sub> atmosphere before the loading procedure. AC supported Fe catalysts were synthesized with and without promoter to investigate the promoter effects. Sequential impregnation and co-impregnation methods were employed. The difference was the impregnation procedure of Mn and Zn promoters. For sequential impregnation, active metal was impregnated to support, then dried and calcined. After the calcination step, promoters were added to the catalyst. For co-impregnation, active metal-Mn or active metal-Zn were added together with an aqueous solution on the support material.

#### 3.2.1 Sequential impregnation

For 10 wt.% nominal loading of iron, iron nitrate was dissolved in deionized water at room temperature. The solution was impregnated dropwise on the AC. While adding the solution, the catalyst was agitated using the flash shaker vibromatic to enhance the dispersion of metal on the support. To further improve the dispersion, the catalyst was

kept in the ultrasonic bath for 15 minutes. After impregnation of iron, the catalyst was dried at room temperature for 4 hours in a desiccator then, the temperature was incrementally increased to 60°C then 80°C, finally 100°C in a vacuum oven. Before adding the promoters, 10Fe was calcined at 350°C under N<sub>2</sub> flow in a tubular furnace for 4 hours. When the calcination was completed, the manganese nitrate for Mn (2 wt.% wrt. catalyst) and copper nitrate for Cu (2 wt.% wrt. catalyst) promoters were impregnated by following the previous loading, drying and calcination steps. tri-Sodium citrate for Na (1 wt.% wrt. catalyst) and potassium nitrate for K (1 wt.% wrt. catalyst) promoters were loaded with the same method. The using of ‘-’ between the metals refers to the sequential impregnation like 10Fe-2Mn.

The sequential impregnation procedure is provided in Figure 3.1 and labeled as M<sub>1</sub> in Table 3.4.

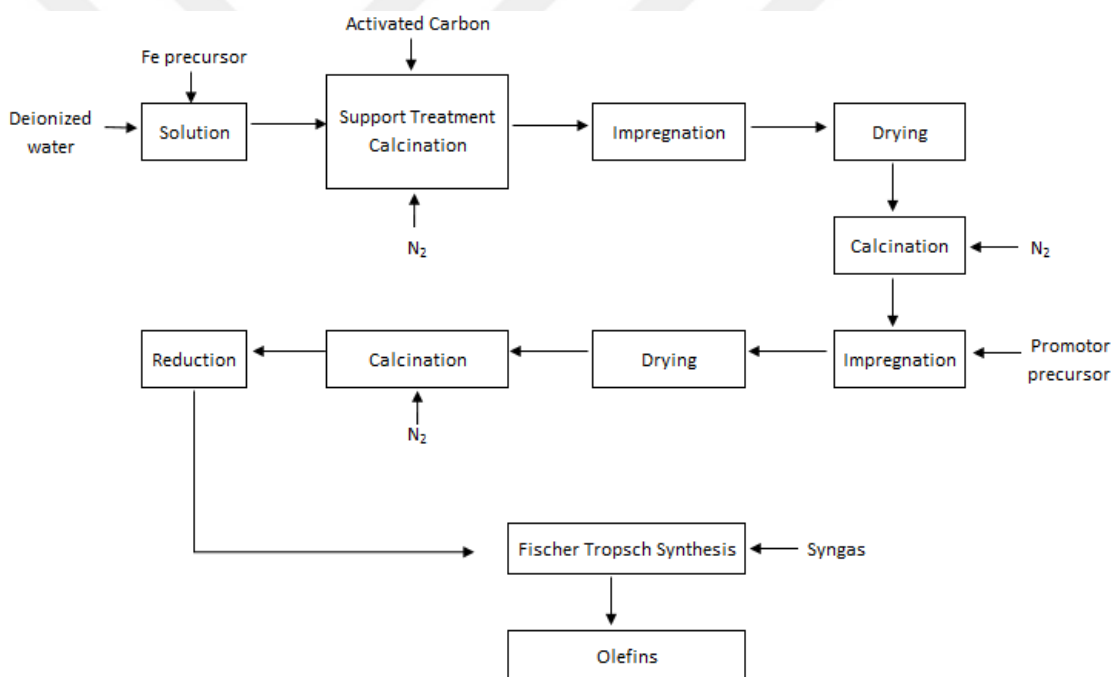


**Figure 3.1** : Sequential impregnation procedure.

### 3.2.2 Co-impregnation

For 10 wt.% nominal loading of Fe; iron nitrate and manganese nitrate precursors for Mn (2 wt.% wrt. catalyst) were dissolved in deionized water separately. Then the solutions were mixed. While adding the solution, the catalyst was agitated by the flash shaker vibromatic to enhance dispersion of metals on the support. The catalyst was kept in the ultrasonic bath for 15 minutes to enhance the dispersion. After the

ultrasonic bath, the sample was dried at room temperature for 4 hours in a desiccator. Subsequently, it was dried with an increased temperature, at 60°C, 80°C and 100°C in a vacuum oven. 10Fe2Zn was synthesized with zinc nitrate hexahydrate (2 wt.% wrt. catalyst) precursor following the same procedure. To prepare 10Fe0.3Na0.1S iron nitrate (10 wt.%), tri-Sodium citrate for Na (3 wt.% wrt. iron) and iron sulfate (1 wt.% wrt. iron) were dissolved separately in deionized water. Then solutions were mixed and impregnated into support. Catalysts were calcined 350°C under N<sub>2</sub> flow in a tubular furnace for 4 hours. 10Fe2Mn and 10Fe2Zn were loaded with Mn (2 wt.% wrt. catalyst), Zn (2 wt.% wrt. catalyst), Na (1 wt.% wrt. catalyst) and K (1 wt.% wrt. catalyst) promoters by sequential impregnation method. Catalysts whose metals were written together refer to co-impregnation like 10Fe2Mn.

Mn and Zn promoters were loaded by co-impregnation. Cu loaded by sequential impregnation because of challenges while preparing it.

The co-impregnation procedure is provided in Figure 3.2 and labeled as M<sub>2</sub> in Table 3.4.

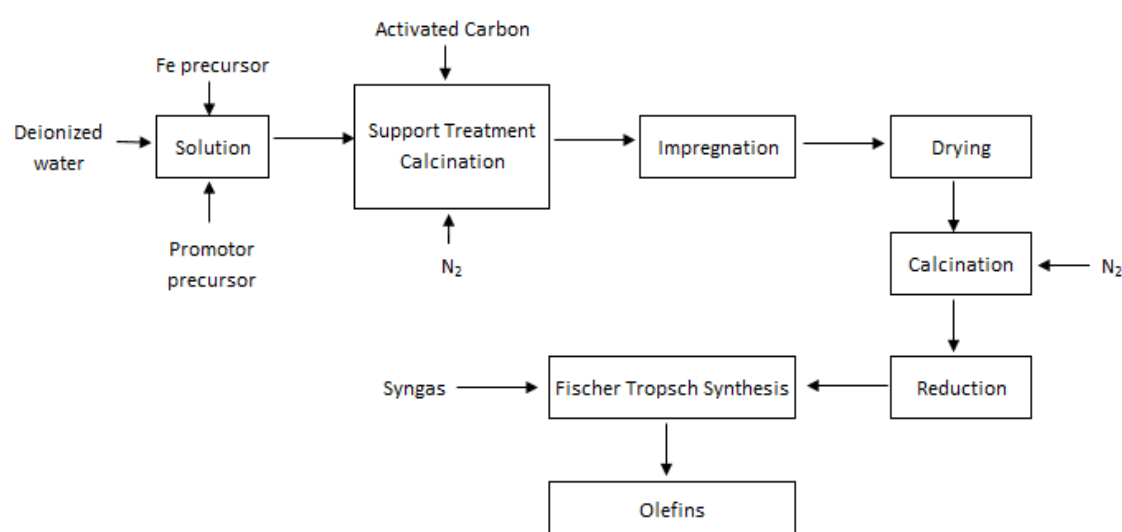


**Figure 3.2 :** Co-impregnation procedure.

The powder form of 10Fe-2Cu-1K catalyst can be seen in Figure 3.3.



**Figure 3.3 :** 10Fe-2Cu-1K catalyst.

Synthesized 16 catalysts with catalyst codes, promoters and synthesis methods of catalysts were listed in Table 3.4. Sequential impregnation is labeled as M<sub>1</sub>. Co-impregnation is labeled as M<sub>2</sub>. For example, 10Fe2Mn-1K indicates that Mn was loaded by M<sub>2</sub> (co-impregnation), K was loaded by M<sub>1</sub> (sequential impregnation).

**Table 3.4 :** Formulation and synthesis method of AC supported catalyst.

Catalyst code	Promoters	Synthesis method
10Fe	-	M <sub>1</sub>
10Fe-2Mn	Mn	M <sub>1</sub>
10Fe2Mn	Mn	M <sub>2</sub>
10Fe2Mn-1K	Mn, K	M <sub>2</sub> , M <sub>1</sub>
10Fe2Mn-1Na	Mn, Na	M <sub>2</sub> , M <sub>1</sub>
10Fe2Mn-2Zn	Mn, Zn	M <sub>2</sub> , M <sub>1</sub>
10Fe2Zn	Zn	M <sub>2</sub>
10Fe2Zn-1K	Zn, K	M <sub>2</sub> , M <sub>1</sub>
10Fe2Zn-1Na	Zn, Na	M <sub>2</sub> , M <sub>1</sub>
10Fe2Zn-2Mn	Zn, Mn	M <sub>2</sub> , M <sub>1</sub>
10Fe-2Cu	Cu	M <sub>1</sub>
10Fe-2Cu-1K	Cu, K	M <sub>1</sub>
10Fe-2Cu-1Na	Cu, Na	M <sub>1</sub>
10Fe-2Cu-2Mn	Cu, Mn	M <sub>1</sub>
10Fe-2Cu-2Zn	Cu, Zn	M <sub>1</sub>
10Fe0.3Na0.1S	Na, S	M <sub>2</sub>

### 3.3 Catalyst Characterization

Synthesized catalysts were characterized using various methods and equipment as listed in Table 3.5.

**Table 3.5** : Methods and equipments used in the characterization of catalysts.

Method	Equipment	Purpose
Scanning Electron Microscope		
Energy Dispersive X-ray (SEM-EDX)	Phenom World	Sample's surface topography
Brunauer-Emmett-Teller (BET)	IGA HIDEN ISOHEMA/WR13701	Determine surface area and pore volume
X-ray Diffraction (XRD)	Rigaku Miniflex600	Crystal structure identification
H <sub>2</sub> -Temperature Programmed Reduction (H <sub>2</sub> -TPR)	IGA HIDEN ISOHEMA/WR13701	Reduction behavior of metal oxides

Scanning Electron Microscope Energy Dispersive X-ray (SEM-EDX) is the surface analytical technique. High resolution images of surface topography which includes the composition of elements are produced. SEM-EDX images of the samples were obtained by Phenom World.

Brunauer-Emmett-Teller (BET) is a theory established by three scientists and explains the physical adsorption of gas molecules on a solid surface then serves it as a measuring technique of specific surface area. Surface area of samples was determined by N<sub>2</sub> physisorption at -195 °C using by Intelligent Gravimetric Analyzer HIDEN ISOHEMA/WR13701 instrument. 45 mg sample was pre-treated by degassing at 150 °C under vacuum.

XRD (X-ray Diffraction) is the identification method of the crystalline structure. The XRD patterns were recorded on Rigaku Miniflex600 equipment using Cu-K $\alpha$  radiation ( $\lambda = 0,154$  nm). The  $2\theta$  angles were scanned between 10-70 °C.

H<sub>2</sub>-Temperature Programmed Reduction (H<sub>2</sub>-TPR) was conducted to estimate reduction properties of oxides to metallic phase by Intelligent Gravimetric Analyzer HIDEN ISOHEMA/WR13701 instrument. Analysis was carried out by heating 100

mg of the calcined catalysts up to 900 °C with a rate of 5 C<sup>o</sup> /min in 50 ml/min H<sub>2</sub>/Ar of a gas mixture of 5% H<sub>2</sub> in Ar.

### 3.4 High Throughput Screening System

All the activity tests were carried out on the AMTECH RS8 High Throughput System (HTS) equipped with 8 parallel fixed bed reactors at Energy Institute of the Scientific and Technological Research Council of Turkey (TUBITAK). The test system is displayed in Figure 3.4. The high throughput system consists of gas supply, gas mix tank, reactors, wax product trap, liquid product trap, gas analyser and control system.

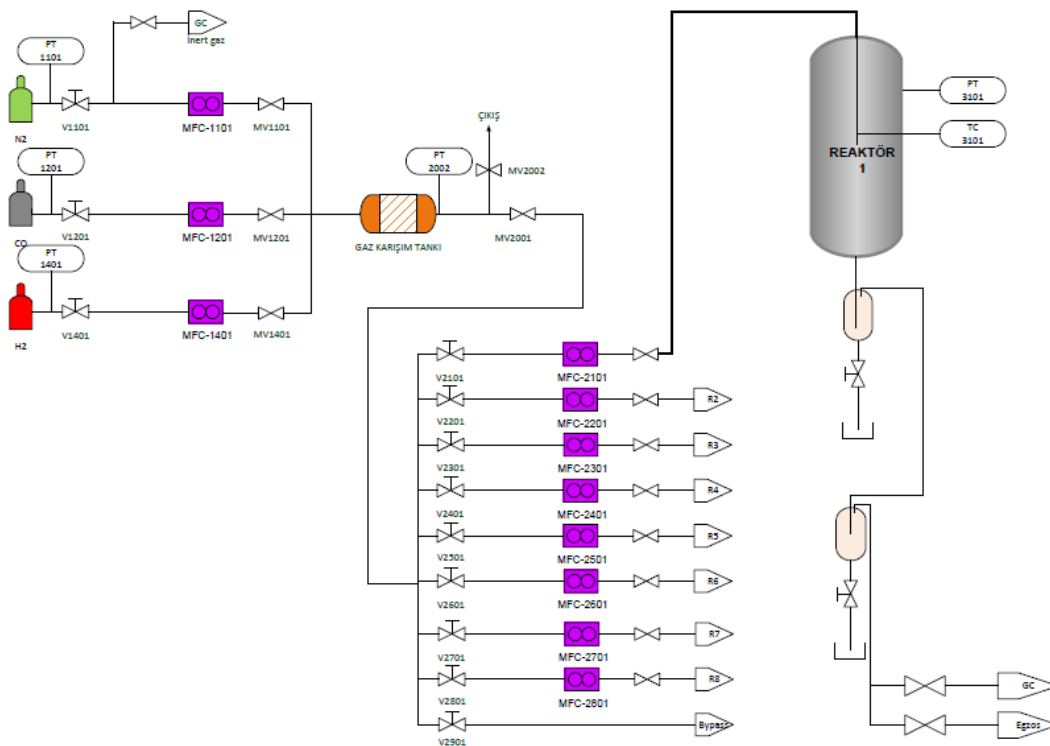


**Figure 3.4 :** High Throughput System.

HTS has 8 fixed bed reactors (ID = 7 mm) which can resist up to 100 bar and 500 °C. The reactors are made from stainless steel SS316L. Fixed bed volume is up to 5 ml of catalyst and the catalyst could be used either in powder or pellet form. Every reactor has its own heating system and the temperature can be set separately for each reactor. The reactor temperatures are measured by a thermocouple that is placed in a catalyst bed and temperatures are set and controlled by AMTECH software. Input and output

lines of the reactor are heated to prevent the condensation in the lines. Backpressure valves that work to control pressure are placed separately for all reactors.

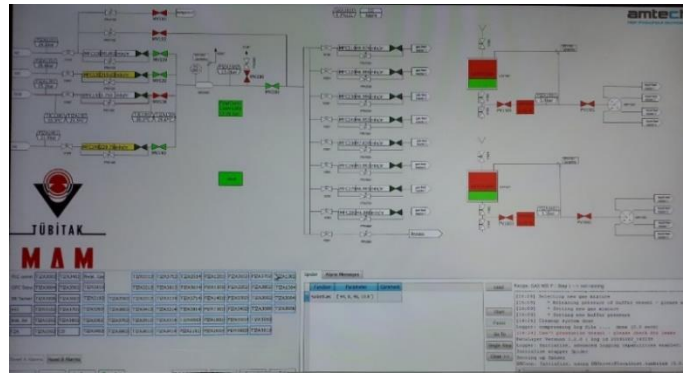
H<sub>2</sub> and CO are mixed in a gas mixing tank with desired ratios. Proportioned syngas is fed to reactors through the MFCs with a certain flow rate. The products flow through the hot pipelines entering the hot trap in which wax products are collected. Then, gaseous products reach to cold trap and the products which condensate at that temperature are collected. To analyze the gas mixture composition the residual product is fed to Gas Chromatography Agilent Technologies 789A. Online GC analyses the products by sampling from each reactor and bypass line. The bypass line is used for analyzing the composition of inlet stream. Using analysis result; conversion, selectivity and product yield etc. are calculated. Figure 3.5 shows the process flow diagram of the high throughput system.



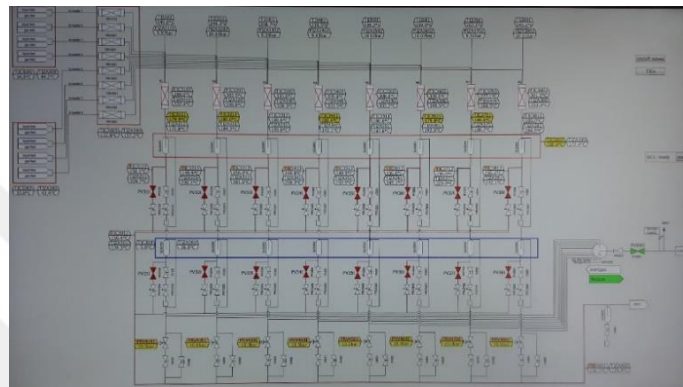
**Figure 3.5 :** Process flow diagram of the high throughput system.

Figure 3.6 shows the AMTECH software. Gas cylinder pressure, H<sub>2</sub>/CO ratio, mix tank pressure, flow rates of each reactor can be set and controlled as it is seen in Figure 3.6 (a). The next one, Figure 3.6 (b) shows that the pressure and temperature of the reactors, the temperature of pipelines, hot trap, cold trap and the backpressure valves values, at the end the line which goes to the GC analyzer.





(a)



(b)

**Figure 3.6 :** (a) Feed and (b) reaction parts of AMTECH software.

The inside (a) and outside (b) view of the reactors can be seen in Figure 3.7. Notched part of the reactor (a) is covered with glass wool to keep the catalyst within the reactor.



(a)

(b)

**Figure 3.7 :** (a) Inside view and (b) outside view of a fixed bed reactor.

### 3.5 Catalyst Test Procedure

The first step of catalyst loading is placing the glass wool in the middle of the reactor to keep the catalyst within the reactor. Then, 0.5 g catalyst, which is diluted with quartz powder (1:1 by volume) to prevent hot spots, was loaded.

The reduction proceeded *in situ* at 350 °C, atmospheric pressure for 4 hours in syngas flow with the H<sub>2</sub>/CO = 2 by volume (H<sub>2</sub>/CO/N<sub>2</sub> = 60/30/10 vol %). When reduction was completed, reactors were cooled down to 200 °C.

Firstly, catalysts were tested at different temperatures and pressures (260 °C-10 bar, 340 °C-10 bar and 340 °C-20 bar) to decide the optimum reaction conditions. While the temperature and pressure were changing, syngas composition was kept constant at H<sub>2</sub>/CO = 1 and gas hourly space velocity (GHSV) was 2000 h<sup>-1</sup>. Regarding the catalytic activity and product distribution, 340 °C-10 bar was chosen. The reasons for that are discussed in Chapter 5.

After deciding on reaction conditions, all tests were carried out at 340 °C and 10 bar. The inlet gas composition was H<sub>2</sub> (45 vol %), CO (45 vol %) and N<sub>2</sub> (10 vol %) with a gas hourly space velocity 2000 h<sup>-1</sup>. Reactions took place almost 160 hours to observe the catalyst stability.

During the reaction, Agilent Technologies 789A Gas Chromatography equipment analyzed the composition of gas products. GC has 8 columns and 3 detectors. One flame ionization detector (FID) and two thermal conductivity detectors (TCD1, TCD2) work for measuring outlet gases. Hydrocarbon products (C<sub>1</sub>-C<sub>6</sub>) are analysed by FID; N<sub>2</sub>, CO<sub>2</sub> and CO gases are analysed by TCD1 and H<sub>2</sub> is analysed by TCD2 detector. The temperature of detectors is 250 °C and total analysis period is 7 min. N<sub>2</sub> and H<sub>2</sub> are used as carrier gases.

### 3.6 Calculations

The activity and selectivity were calculated using the GC data which includes inlet and outlet stream of reaction. CO conversion was calculated on a carbon atom basis by nitrogen normalization assuming that the amount of nitrogen has remained constant during the reaction. The equation is:

$$X_{CO} = \frac{F_{CO_{inlet}} - F_{CO_{outlet}}}{F_{CO_{inlet}}} \times 100\% \quad (7)$$

where  $X_{CO}$  represents the CO conversion,  $CO_{inlet}$  and  $CO_{outlet}$  are the molar flow rate of the CO at the inlet and outlet.

CO<sub>2</sub> selectivity was calculated as follows:

$$S_{CO_2} = \frac{F_{CO_2_{outlet}}}{F_{CO_{inlet}} - F_{CO_{outlet}}} \times 100\% \quad (8)$$

where  $F_{CO_2_{outlet}}$  is the molar flow rate of the CO<sub>2</sub> at the outlet stream and  $S_{CO_2}$  refers to the selectivity of CO<sub>2</sub>.

Hydrocarbon selectivity values were calculated on a carbon basis taking account of the CO<sub>2</sub>-free reaction since CO<sub>2</sub> is not a hydrocarbon product. The selectivity of each hydrocarbon product was calculated according to:

$$S_{C_nH_m} = \frac{(n) (F_{C_nH_m_{outlet}})}{F_{CO_{inlet}} - F_{CO_{outlet}} - F_{CO_2_{outlet}}} \times 100\% \quad (9)$$

where  $S_{C_nH_m}$  is the selectivity of any products.  $F_{C_nH_m_{outlet}}$  is the molar flow rate of an individual hydrocarbon at the outlet stream. Subtitles, n is the carbon number, m is the hydrogen number of the product.

Olefin yield was calculated to find olefin production per gram iron per second. It was calculated on a carbon atom basis.

$$\text{Olefin yield} = \frac{(\sum_{i=2}^4 F_{C_i_{outlet}}) (n) (MW_C)}{g_{Fe} 3600} \quad (10)$$

where  $F_{C_{ioutlet}}$  is the molar flow rate of the olefin product, n is the carbon number and  $MW_C$  is the molecular weight of carbon.  $g_{Fe}$  is the amount of iron which is active metal.



## 4. RESULTS AND DISCUSSION

The main purpose of this thesis is screening of different catalysts for high C<sub>2</sub>=C<sub>4</sub> olefin selectivity, olefin/paraffin (O/P) ratio with a high CO conversion. Catalysts were tested in a high throughput screening system to investigate their performance and behavior for FTO reaction. Scanning Electron Microscope Energy Dispersive X-ray (SEM-EDX), Brunauer-Emmett-Teller (BET), X-Ray Diffraction (XRD) and Temperature Programmed Reduction (H<sub>2</sub>-TPR) analyses were performed for catalyst characterizations; surface composition, surface area, crystalline structure and reduction profile of catalysts.

### 4.1 Structural Properties of Catalysts

SEM-EDX analysis was performed for determining the surface topology and composition of catalysts. To measure the surface area of catalysts BET analysis was used. XRD analysis was done to examine the crystalline structure of metals and H<sub>2</sub>-TPR was performed to determine the reduction profile of catalysts.

#### 4.1.1 SEM-EDX

SEM-EDX was conducted on support AC and calcined catalysts (10Fe, 10Fe2Zn-1K and 10Fe-2Cu-1K) with low-magnification except 10Fe catalyst. Figure 4.1 shows SEM-EDX images of (a) unloaded AC, (b) 10Fe, (c) 10Fe2Zn-1K and (d) 10Fe-2Cu-1K. SEM-EDX image of 10Fe was obtained with high-magnification which can be seen in pink window in Figure 4.1 (b). Particle size of AC and also prepared catalysts were in range 0-200 $\mu$  and SEM analyse were performed without sieving samples. In Figure 4.1 (a), a trace amount of Si and O elements were found in unloaded AC. This was associated with SiO<sub>2</sub> which could be a residue from the industrial synthesis of AC. As it is seen in Figure 4.1 (b), SEM-EDX image of 10Fe, Fe (10 wt.%) particles were uniformly distributed in AC. Different size of carbon particles and metal (brighter particles) were observed on 10Fe2Zn-1K and 10Fe-2Cu-1K surfaces which were shown in Figure 4.1 (c) and (d) respectively.

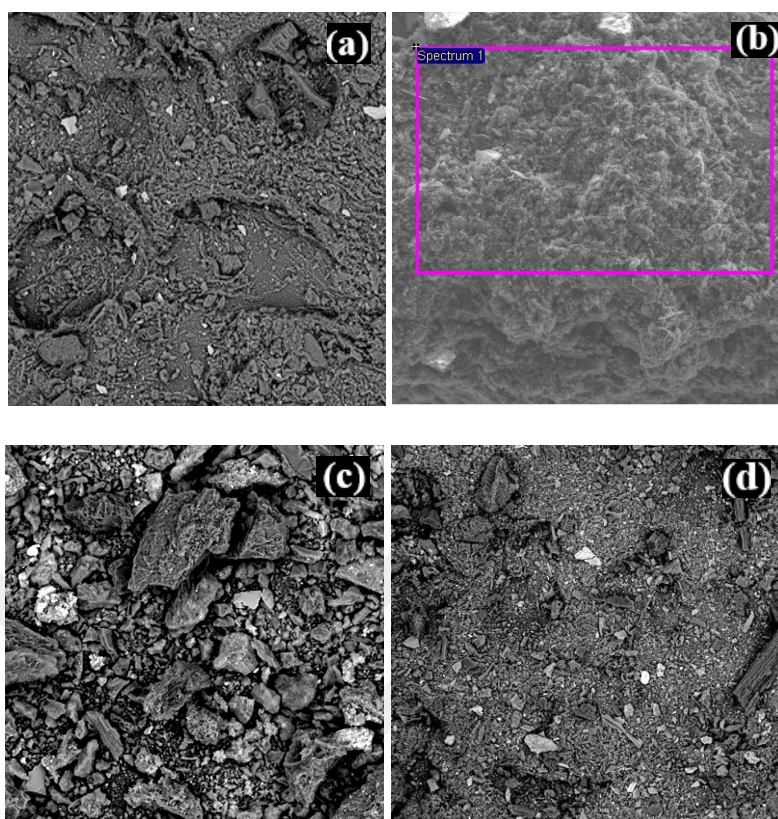


**Figure 4.1** : SEM-EDX images of (a) unloaded AC, (b) 10Fe, (c) 10Fe<sub>2</sub>Zn-1K, (d) 10Fe-2Cu-1K.

Table 4.1 shows weight concentration of elements which were determined by EDS. C, Si and O concentrations of AC were 81.21, 1.07 and 17.71 wt.% respectively. For 10Fe catalyst, weight concentration of C and Fe were 81.21 and 9.22 wt.% respectively. Iron concentration was close to the nominal loading of Fe (10 wt.%). Fe loading of 10Fe<sub>2</sub>Zn-1K and 10Fe-2Cu-1K was 13.96 wt.% and 11.70 wt.% respectively. These higher amount of loadings could be caused by sample chosen from a region that the iron accumulated. However, Fe loadings were close to the desired amount. Nominal loadings of Zn, Cu and K were 2, 2 and 1 wt.% respectively. Zn and K loadings of 10Fe<sub>2</sub>Zn-1K catalyst were 2.22 and 1.13 wt.% respectively which were in line with the desired amount. Cu and K loadings of 10Fe-2Cu-1K catalyst were 2.67 and 0.87 wt.% respectively which are close to the desired amount.

**Table 4.1** : Weight concentration (wt.%) of samples according to SEM-EDX.

Sample	C	Fe	Zn	Cu	K	Si	O
AC	81.21	-	-	-	-	1.07	17.71
10Fe	75.46	9.22	-	-	-	2.16	13.16
10Fe2Zn-1K	75.12	13.96	2.22	-	1.13	0.95	6.62
10Fe-2Cu-1K	77.23	11.70	-	2.67	0.87	1.35	6.17

#### 4.1.2 BET

Surface areas of the calcined samples were obtained through BET analysis by N<sub>2</sub> physisorption starting with degassing treatment of 45 mg sample [7]. Surface area of samples are listed in Table 4.2. The surface area of AC was 755.9 m<sup>2</sup>/g. After 10 wt. % Fe loading on AC the surface area declined by 10% to 678.2 m<sup>2</sup>/g. The surface area of Mn, Zn and Cu introduced catalysts were about 12%, 8% and 6% lower than the 10Fe. The decrease in the surface area suggests either that the metal particles block the pore entrances or that pores are filled with metal [43]. Na addition resulted in a decrease in surface area as expected. The surface area of 10Fe-2Cu was 636.7 m<sup>2</sup>/g, then it decreased to 616.0 m<sup>2</sup>/g with Na addition. Also, addition of Na and S on 10Fe decreased the surface area from 678.2 to 649.9 m<sup>2</sup>/g. Interestingly, the surface area of K promoted catalysts, 10Fe2Zn-1K and 10Fe2Cu-1K increased from 620.8 to 664.7 m<sup>2</sup>/g and from 636.7 to 651.9 m<sup>2</sup>/g respectively. The increments were about 7% for 10Fe2Zn-1K and %2 for 10Fe-2Cu-1K. Cheng et al. [15] found that loading 0.50-2 wt. % K on Fe/rGO between caused an increase in BET surface area from 126 to 145 m<sup>2</sup>/g. Suggested reason was the intercalation of potassium precursor (KCO<sub>3</sub>) into graphene layers under ultrasonication. Since the ultrasonic bath was used to synthesize the catalysts in this study, increase in surface area with K additive could be caused by the intercalation of K into AC.

**Table 4.2** : Surface area of catalysts.

Catalyst	Surface area (m <sup>2</sup> /g)	Catalyst	Surface area (m <sup>2</sup> /g)
AC	755.9	10Fe2Mn-1K	488.2
10Fe	678.2	10Fe2Zn-1K	664.7
10Fe2Mn	596.8	10Fe-2Cu-1K	651.9
10Fe2Zn	620.8	10Fe-2Cu-1Na	616.0
10Fe-2Cu	636.7	10Fe0.3Na0.1S	649.9

### 4.1.3 XRD

XRD analysis was conducted to determine the crystalline structure of calcined 10Fe, 10Fe2Zn, 10Fe2Zn-1K, 10Fe-2Cu, 10Fe-2Cu-1K and 10Fe-2Cu-1Na catalysts and 10Fe-2Cu-1K after reaction 160 h reaction. The AC and iron oxide phases were investigated. A sharp AC peak was observed at  $2\theta$  value of  $26.6^\circ$  in all XRD patterns.  $\text{Fe}_2\text{O}_3$  (hematite) and  $\text{Fe}_3\text{O}_4$  (magnetite) were iron oxides phases that formed in catalysts after calcination. In Figure 4.2 and Figure 4.3,  $\text{Fe}_2\text{O}_3$  peaks were observed at  $24.3^\circ$ ,  $33.1^\circ$ ,  $40.9^\circ$ ,  $49.5^\circ$ ,  $54.1^\circ$ ,  $57.6^\circ$  and  $64.1^\circ$ .  $\text{Fe}_3\text{O}_4$  peaks were detected at  $30.1^\circ$ ,  $35.6^\circ$ ,  $43.1^\circ$ , and  $62.5^\circ$ .  $2\theta$  values of peaks were determined by using International Centre for Diffraction Data. Observing  $\text{Fe}_3\text{O}_4$  peaks on calcined AC supported catalysts attributed to that partial oxidation of the carbon support by released oxygen during the nitrate decomposition helped the partial reduction of iron to  $\text{Fe}_3\text{O}_4$  instead of keeping it at  $\text{Fe}_2\text{O}_3$  phase [5].

XRD patterns of 10Fe, 10Fe-2Cu, 10Fe-2Cu-1K, 10Fe-2Cu-1Na catalysts were plotted in Figure 4.2. After addition of promoters to 10Fe catalyst, the size of  $\text{Fe}_2\text{O}_3$  diffraction peak at  $33.1^\circ$  significantly increased as it is seen in Figure 4.2. The same increase was observed on the size of  $\text{Fe}_3\text{O}_4$  diffraction peak at  $35.6^\circ$ . These results can be attributed to forming iron oxides in each calcination step and particle size growth because of the heat treatment during calcination.

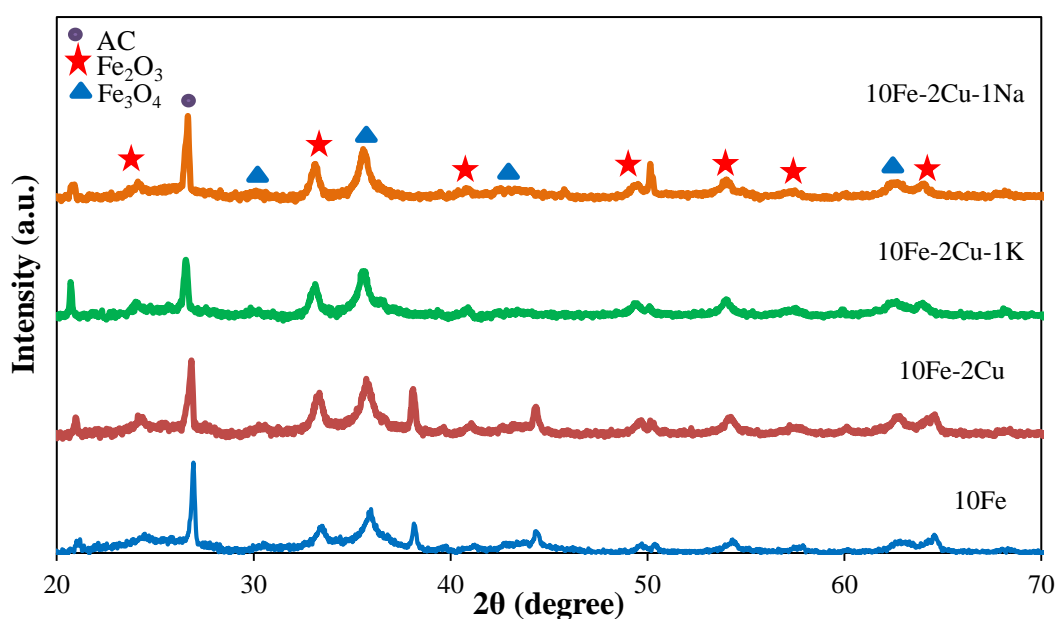


**Figure 4.2 :** XRD patterns of calcined 10Fe, 10Fe-2Cu, 10Fe-2Cu-1K and 10Fe-2Cu-1Na catalysts.



No diffraction peaks attributable to Cu-containing or K-containing phases were observed in Figure 4.2. This is possibly due to low concentration of these elements in the catalysts [44].

In Figure 4.3, XRD patterns of calcined 10Fe, 10Fe2Zn and 10Fe2Zn-1K catalysts are shown. Diffraction peaks of  $\text{Fe}_2\text{O}_3$  and  $\text{Fe}_3\text{O}_4$  were observed at the same  $2\theta$  values as indicated for Cu promoted catalysts in Figure 4.2. Zn addition on 10Fe resulted in a significant increase in diffraction peak size of  $\text{Fe}_3\text{O}_4$  at  $2\theta$  value of  $30.1^\circ$  and  $35.6^\circ$  in Figure 4.3. This increase in the peak size confirms that  $\text{Fe}_3\text{O}_4$  formed after calcination in AC supported Fe catalysts. Zn-containing or K-containing oxides were not observed in XRD patterns. The low concentration of Zn and K in catalysts led to this possibly [44].

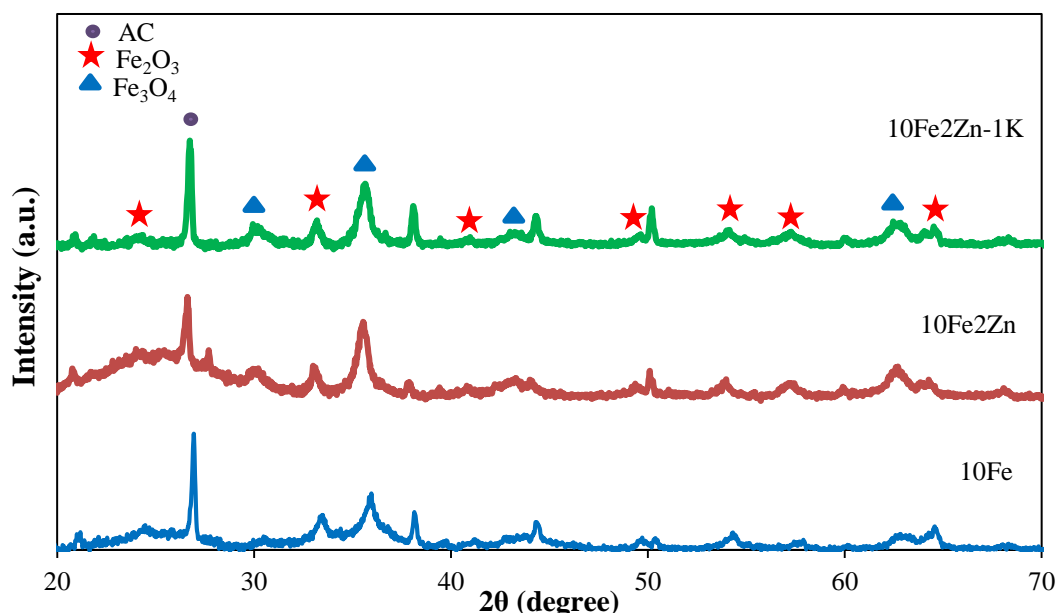


**Figure 4.3 :** XRD patterns of calcined 10Fe, 10Fe2Zn and 10Fe2Zn-1K catalysts.

Figure 4.4 shows XRD patterns of calcined 10Fe-2Cu-1K catalyst and its used form.  $\text{Fe}_2\text{O}_3$  and  $\text{Fe}_3\text{O}_4$  phases converted into FeO and  $\text{Fe}_3\text{C}$  after the reaction. Fe reduction was proven by forming of FeO from  $\text{Fe}_2\text{O}_3$  and  $\text{Fe}_3\text{O}_4$  phases. FeO phase was observed at  $2\theta$  values of  $36.7^\circ$  and  $42.7^\circ$ . Iron carbide  $\text{Fe}_3\text{C}$  diffraction peaks phase was observed at  $2\theta$  values of  $40.1^\circ$ ,  $42.9^\circ$ ,  $45.6^\circ$  and  $68.1^\circ$ . Fe carbide phase forming during the reaction is consistent with literature since iron carbides are active phases for FT [33, 45]. C (graphite) peaks were detected at  $2\theta$  values of  $54.8^\circ$  and  $59.7^\circ$ . Observing C (graphite) indicates that carbon deposition occurred in 10Fe-2Cu-1K catalyst for 160 h reaction. Diffraction peaks of  $\text{SiO}_2$  phase also detected in XRD pattern in used

catalyst since catalysts were diluted with quartz powder (1:1 by volume) which was explained in Chapter 3.

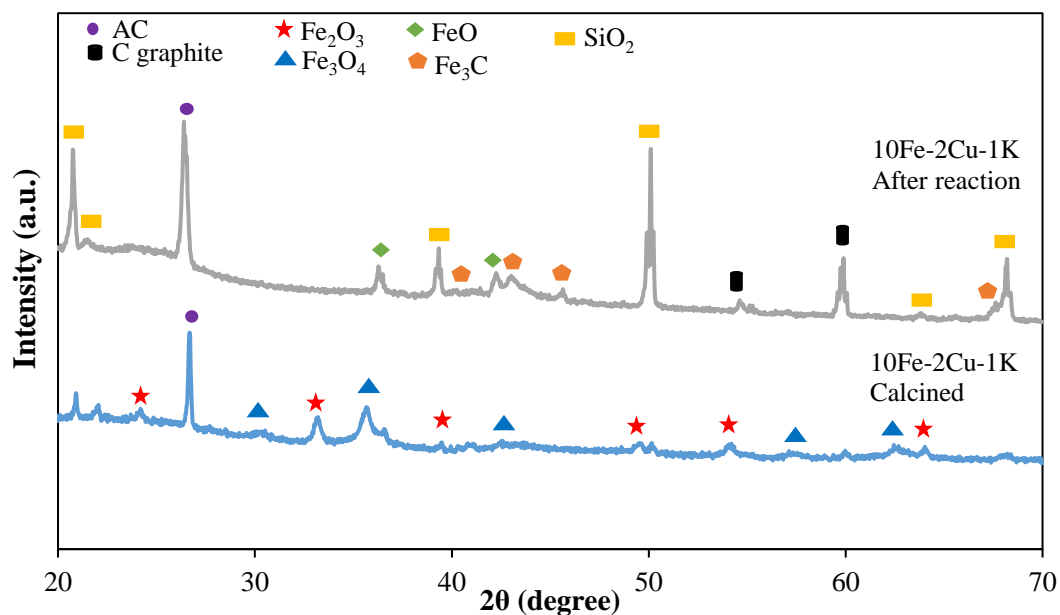


**Figure 4.4 :** XRD patterns of calcined 10Fe-2Cu-1K and after reaction 10Fe-2Cu-1K.

#### 4.1.4 H<sub>2</sub>-TPR

Reduction profiles of calcined 10Fe, 10Fe-2Cu, 10Fe-2Cu-1K and 10Fe2Zn-1K catalysts were determined by H<sub>2</sub>-TPR using IGA. The instrument produces curves giving H<sub>2</sub> concentration/flowrate in terms of MS signal as a function of temperature. Figure 4.5 shows the H<sub>2</sub>-TPR profile of catalysts. Two main groups of hydrogen consumption peaks were observed for 10Fe catalyst. First temperature region 350–600°C is related to the formation of FeO from Fe<sub>2</sub>O<sub>3</sub> phase. In this region, hydrogen consumption at ~500°C is related to the reduction of Fe<sub>3</sub>O<sub>4</sub> to FeO. Second peak 600–750 °C can be attributed to the reduction of FeO to metallic iron Fe. This is in agreement with the findings of [39, 42, 46].

Addition of Cu to 10Fe, significantly shifted the reduction peaks to lower temperatures compared to 10Fe catalyst in Figure 4.5. Reduction proceed between 350-750 °C of 10Fe catalyst whereas reduction profile of 10Fe-2Cu proceed between 210-700 °C [42]. It is well known that CuO is easily reduced at lower temperature in H<sub>2</sub> atmosphere [47]. As CuO reduces, Cu crystallites provide H<sub>2</sub> dissociation sites, which in turn lead to reactive hydrogen species capable of reducing iron oxides at relatively low temperatures. Therefore, the addition of Cu promotes the reduction of iron-based catalyst in H<sub>2</sub> atmosphere. For 10Fe-2Cu catalyst, a small peak at 210 °C was observed

and it can be attributed to the reduction of both  $\text{Fe}_2\text{O}_3$  to  $\text{Fe}_3\text{O}_4$  and  $\text{CuO}$  to  $\text{Cu}$ . Even though  $\text{CuO}$  phase was not detected in XRD patterns in Figure 4.2 because of low Cu content, observing  $\text{CuO}$  reduction in  $\text{H}_2$ -TPR can be possible for calcined 10Fe-2Cu catalyst. Because Cu can change its form to  $\text{CuO}$  during calcination.  $\text{H}_2$  consumption of 10Fe-2Cu catalyst until 600 °C is related to reduction of  $\text{Fe}_2\text{O}_3$  to  $\text{FeO}$  and following reduction to metallic Fe at ~700 °C.

Wan et al. [47] reported that K addition on Cu-Fe catalyst suppressed the reduction of  $\text{Fe}_2\text{O}_3$  to  $\text{Fe}_3\text{O}_4$  in  $\text{H}_2$  atmosphere. It may be due to the inhibiting effect of alkali metals on the  $\text{H}_2$  adsorption [38]. However, K promotion on 10Fe-Cu did not suppress the reduction of iron in this study. In Figure 4.5, for the first reduction peak at 210 °C of 10Fe-2Cu-1K there was essentially no effect of K compared to 10Fe-2Cu.

It appears that K promoter on 10Fe-2Cu shifted the second reduction peak from ~700 to 630 °C of the iron catalyst to lower temperatures in Figure 4.5. Zhang et al. [48] observed the same reduction profile on silica supported catalyst. The ease of reduction was attributed to the synergistic effect of Cu and K combination which improve the reduction of catalyst. This synergistic effect of Cu and K might be occurred in 10Fe-2Cu-1K catalyst.

Zhang et al. [44] reported that addition of Zn and K on unsupported iron catalyst shifted the reduction profile to higher temperature. However 10Fe-2Zn-1K catalyst exhibited a similar profile with 10Fe. This can be caused by using AC as a support material in this study whereas Zhang et al. [44] synthesized the unsupported Fe catalyst. This profile can be caused the support interaction with metals Zn and K.

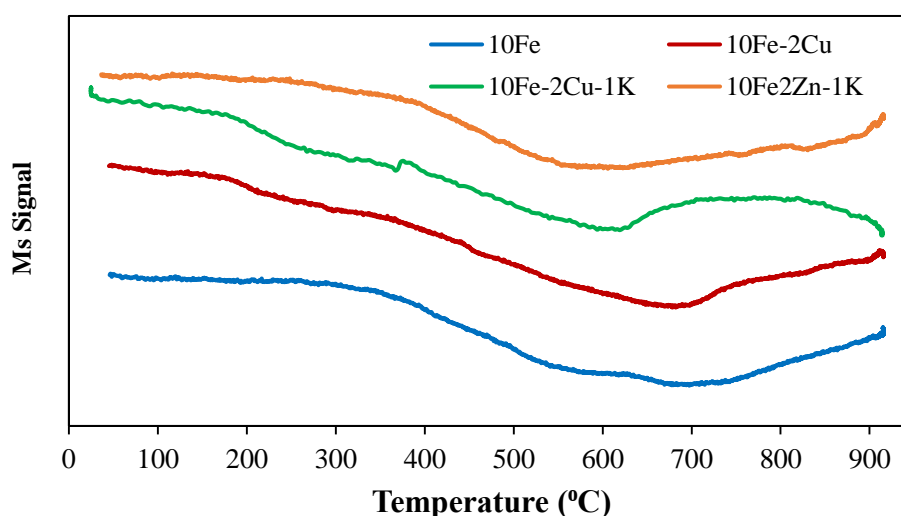


**Figure 4.5 :**  $\text{H}_2$ -TPR curves of 10Fe, 10Fe-2Cu, 10Fe-2Cu-1K and 10Fe-2Zn-1K catalysts.

## 4.2 Catalytic Performance

16 catalysts were synthesized using Fe (active metal), AC (support) and promoters (Mn, Zn, Cu, K, Na and S). Promoter combinations were employed on activated carbon supported iron catalysts. Firstly, 10Fe, 10Fe-2Mn, 10Fe2Mn, 10Fe2Zn and 10Fe-2Cu were investigated. Promoters continued to be added on the purpose of improving the catalyst activity and selectivity to light olefins.

### 4.2.1 Effects of temperature and pressure on catalytic activity and selectivity to light olefins

It is of utmost importance to determine optimum reaction conditions. Hence, synthesized catalysts 10Fe and 10Fe-2Mn, which were explained in Chapter 3, were tested at three consecutive steps starting at 260 °C and 10 bar for 20 h. Then the temperature was increased to 340 °C at 10 bar. At the final step the pressure was increased to 20 bar at constant temperature of 340 °C. CO conversion and olefin selectivity were observed for every different condition. Figure 4.3 shows (a) CO conversion and (b) the light olefins selectivity of 10Fe and 10Fe-2Mn.

CO conversion reached almost 16% for both catalysts at 260 °C and 10 bar for 24 h. To understand if the further increase in temperature has any effect on the conversion, temperature was increased to 340 °C. CO conversion of 10Fe catalyst increased to 37% but quickly lost its activity and reached 16%. The conversion of 10Fe-2Mn was not significantly affected by temperature increase. Pressure was increased from 10 bar to 20 bar to observe its effect on conversion and selectivity. CO conversion was increased at high pressure as expected. However, it had a decreasing effect on selectivity as it is seen in Figure 4.6 (b).

In Figure 4.6 (b) light olefins selectivity of 10Fe decreased from 30% to 3% at 260 °C and 10 bar. The light olefins selectivity of 10Fe-2Mn was around 1%. When the temperature was increased to 340 °C, light olefins selectivity of 10Fe-2Mn was increased. Increase in pressure from 10 to 20 at constant temperature 340 °C was not favorable on the light olefin selectivity.

According to experimental results, 340 °C and 10 bar were chosen as the optimum FTO condition and it is in agreement with literature [3, 38].

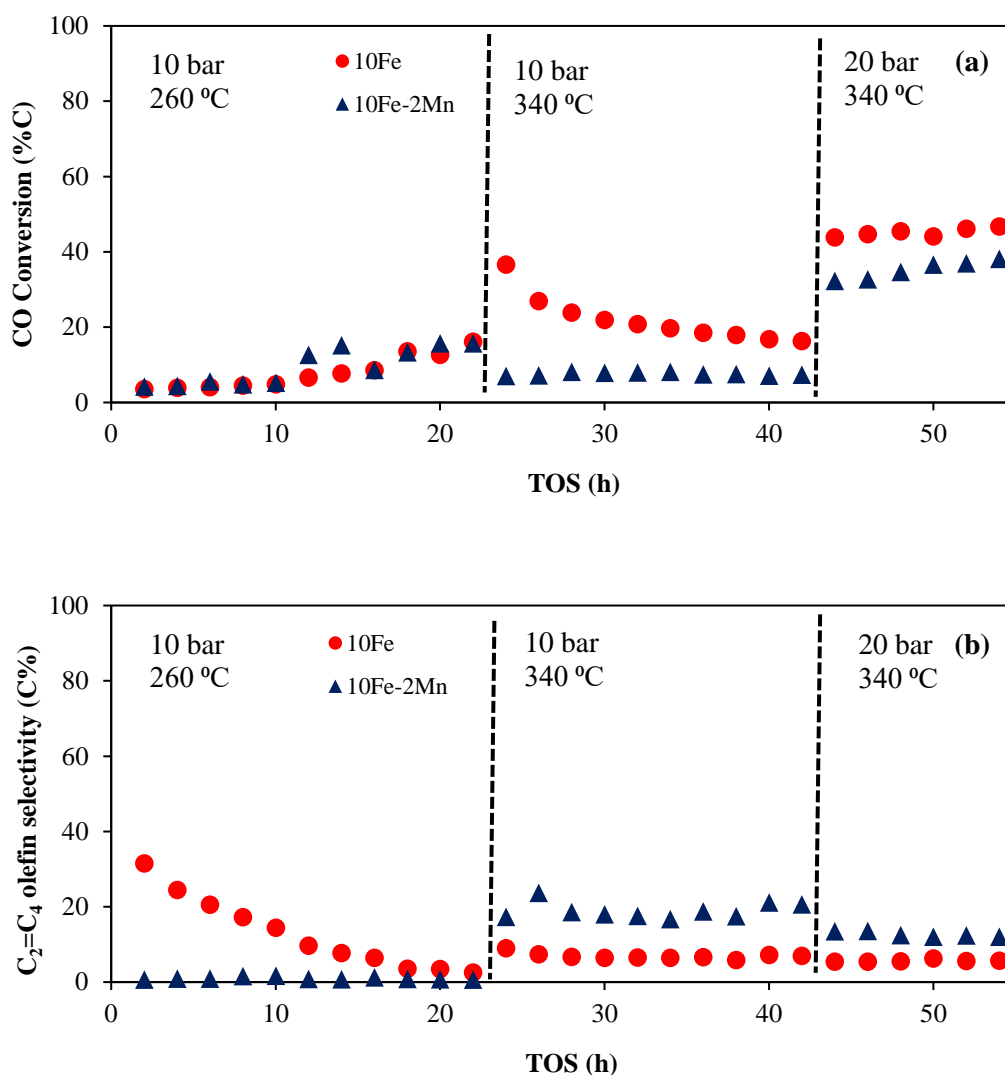


**Figure 4.6 :** (a) CO conversion and (b) light olefins selectivity of 10Fe and 10Fe-2Mn catalysts at different reaction conditions,  $H_2/CO = 1$ ,  $GHSV=2000\text{ h}^{-1}$ .

#### 4.2.2 10Fe catalyst behavior under FTO conditions

10Fe catalysts were synthesized with nominal 10 wt.% iron loading as described in Chapter 3. It was tested at 340 °C 10 bar,  $H_2/CO = 1$  and  $GHSV\ 2000\text{ h}^{-1}$  for 160 h. CO conversion was 35% after 160 h reaction. But, there was no obvious difference in the product selectivity. Figure 4.7 shows the product distribution of 10Fe.  $CO_2$  selectivity was between 20-25% and selectivity to  $CH_4$ ,  $C_2-C_4$  and light olefins ( $C_2=C_4$ ) were 20 % for each product as it is seen in Figure 4.7. Also, light olefins yield of 10Fe was only  $0.5 \times 10^{-3}\text{ gC/g}_{Fe.s}$  for 160 h reaction. Various metals have been investigated as possible promoters to improve FTO activity and the selectivity to olefins.

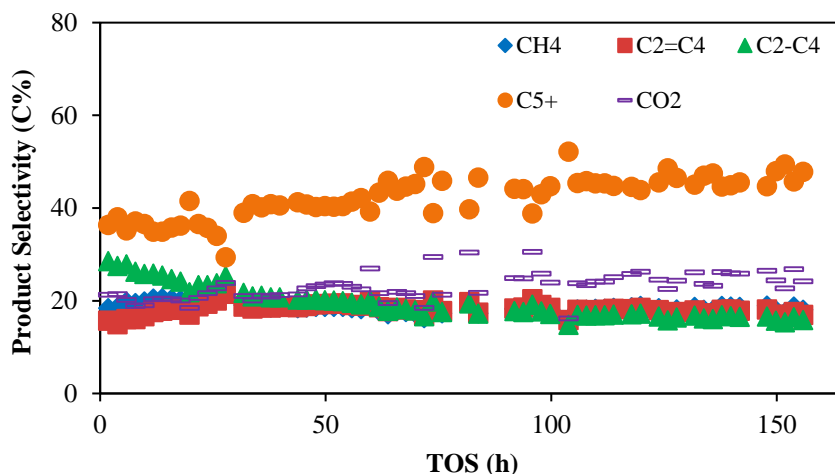


**Figure 4.7 :** Product selectivity of 10Fe.

#### 4.2.3 Promoter effect of Mn on olefin selectivity and synthesis method effect on yield

2 wt.% Mn was added to 10Fe catalyst and its effect on FTO activity and olefin selectivity was investigated. CO conversion and light olefins selectivity of 10Fe and 10Fe-2Mn catalysts were given in Figure 4.6 (a) and (b) respectively. As it is seen in Figure 4.6 (a) at 340 °C–10 bar, CO conversion of 10Fe-2Mn catalyst was significantly lower than 10Fe. The stability of the catalyst was increased with the addition of Mn, thus the rapid decrease observed with 10Fe catalyst was not observed on 10Fe-2Mn and approximately the same conversion values were obtained for 20 h.

In Figure 4.6 (b) at 340 °C–10 bar, it is seen that Mn addition has a positive effect for light olefins production. The addition of Mn to 10Fe catalyst increased the light olefins selectivity by approximately 2.5 times at 340 °C and 10 bar, in Figure 4.6 (b). Similar results were found in the literature. Asami et al. [13] and Tian et al. [14] reported that Mn increased olefin selectivity by suppressing further hydrogenation.

To examine the effect of catalyst preparation on performance and selectivity, Mn promoted catalysts were prepared by two different methods. The first one was sequential impregnation and the other one was co-impregnation as described in Chapter 3. Figure 4.8 shows how the preparation method affected the light olefins yield. Light olefins yield improved for 20 h of reaction from  $1.8 \times 10^{-4}$  to  $4.4 \times 10^{-4}$   $\text{gC/g}_{\text{Fe.s}}$  by changing the synthesis method from sequential impregnation (10Fe-2Mn) to co-impregnation (10Fe2Mn) as it is seen in Figure 4.8. Co-impregnation resulted in

an increase in olefin yield. It has been associated with co-impregnated catalyst being exposed to less heat treatment procedure since one calcination step was skipped. The heat treatment results in sintering of iron particles thus losing the active metal sites [42]. Since co-impregnated 10Fe2Mn catalysts being exposed to less heat treatment, it did not lose active metal sites as sequential impregnated 10Fe-2Mn did.

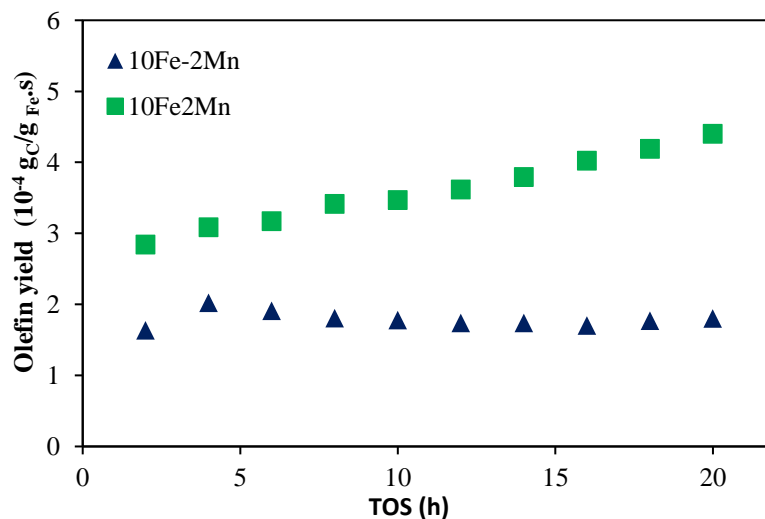


**Figure 4.8 :** Light olefins yield of 10Fe-2Mn and 10Fe2Mn catalysts.

#### 4.2.4 Promoter effects of Mn, Zn and Cu on AC supported Fe catalyst

2 wt.% Mn, Cu and Zn were added to 10Fe catalyst and their effect on FTO activity and selectivity to light olefins, CH<sub>4</sub> and other hydrocarbons were investigated. 10Fe2Mn, 10Fe2Zn and 10Fe-2Cu catalysts were prepared by the methods described in Chapter 3. CO conversion, selectivity towards light olefins, CO<sub>2</sub> and CH<sub>4</sub> were plotted in Figure 4.9. The data blank between 80-100 h caused by the GC as it did not analyze due to carrier gas error.

Figure 4.9 shows (a) CO conversion, (b) light olefins, (c) CO<sub>2</sub> and (d) CH<sub>4</sub> selectivity of catalysts. As it is seen in Figure 4.9 (a), Zn addition improved CO conversion whereas 10Fe2Zn had the highest conversion with a value of 65%. This result is consistent with the literature. Zhao et al. [49] reported that they obtained high CO conversion and by addition alkali promoter to catalyst they obtained high olefin selectivity in FTO reaction with FeZn (1/1mol) bulk catalyst. In literature it was reported that Cu enhanced the reduction of Fe [18, 39, 47]. Reduction effect of Cu was observed in H<sub>2</sub>-TPR profiles of 10Fe and 10Fe-2Cu catalysts in Figure 4.5. Because

of the effect of Cu on reduction, 10Fe-2Cu catalyst had higher initial activity than Mn promoted catalyst. After 50 h, CO conversion of 10Fe2Mn and 10Fe-2Cu are almost the same value in Figure 4.9 (a). The average selectivity to light olefins of 10Fe2Mn, 10Fe2Zn and 10Fe-2Cu were 22%, 15% and 19%, respectively as it is seen in Figure 4.9 (b). Mn promoted had a high selectivity to olefins relatively since Mn suppresses the further hydrogenation of olefins. Competitive H<sub>2</sub> adsorption on Mn decreased H<sub>2</sub>/CO ratio on active sites and this reduces the possibility of further hydrogenation of olefins [14]. In Figure 4.9 (c), CO<sub>2</sub> selectivity of 10Fe2Zn catalyst increased from 30% to 40%. The highest conversion and increased CO<sub>2</sub> selectivity of 10Fe2Zn can be attributed to WGS activity of catalyst [50]. Focusing on Figure 4.9 (c) and Figure 4.9 (d), CO<sub>2</sub> selectivity of 10Fe-2Cu was the lowest value 25% whereas selectivity to CH<sub>4</sub> relatively higher with a value of 20% among three catalysts. Figure 4.9 (d) shows Zn promoted catalyst had the lowest selectivity to CH<sub>4</sub> with a value of 15%.

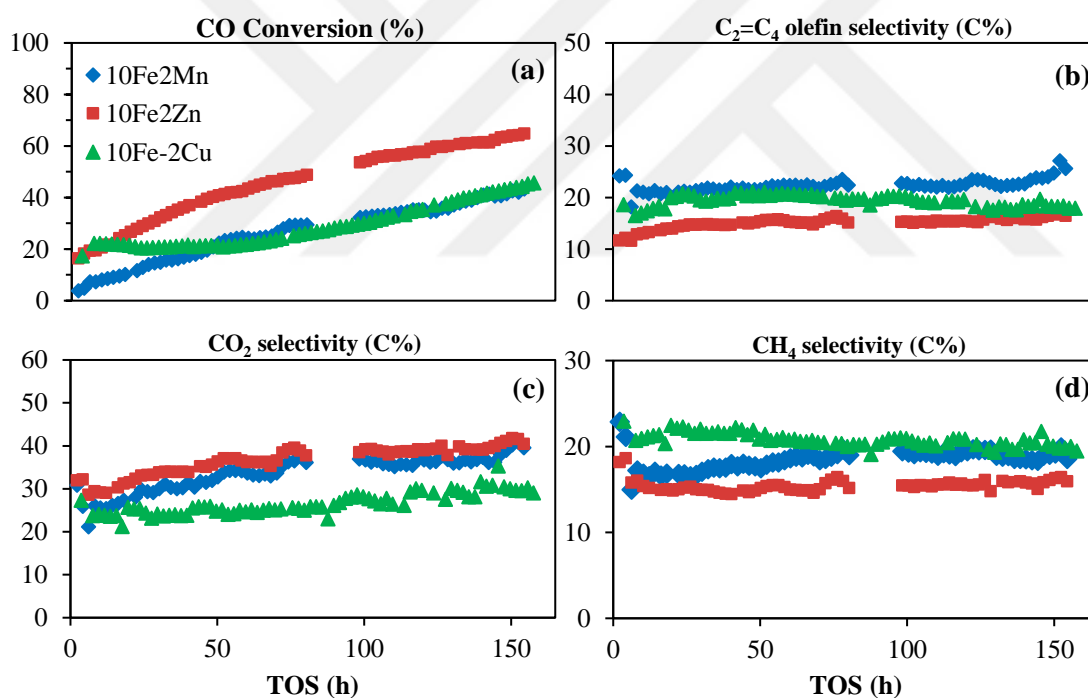


**Figure 4.9 :** (a) CO conversion, (b) light olefins, (c) CO<sub>2</sub> and (d) CH<sub>4</sub> selectivity of Mn, Zn and Cu promoted catalysts at 340 °C, 10 bar, H<sub>2</sub>/CO = 1, GHSV=2000 h<sup>-1</sup>.

Figure 4.10 shows the O/P ratio of Mn, Zn, and Cu promoted catalysts. According to Figure 4.10, 10Fe2Mn had the highest O/P ratio (2.0) which exhibited high selectivity to olefins and low selectivity to paraffins among these three catalysts. O/P ratio of 10Fe2Zn and 10Fe-2Cu were almost 1.0.



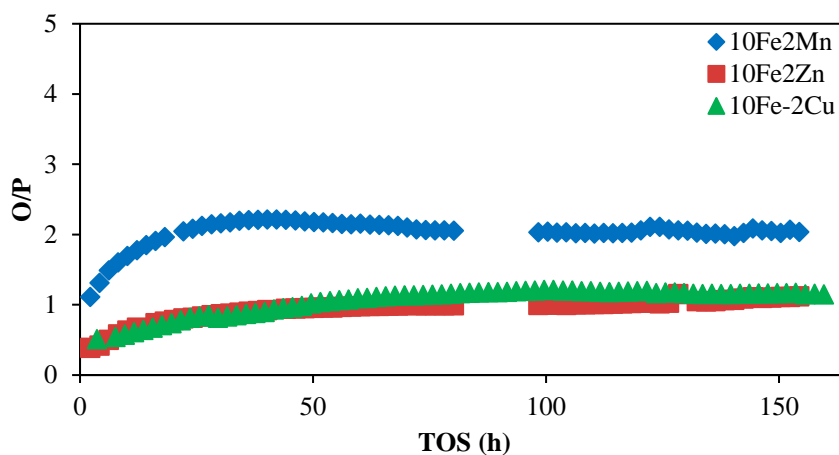


**Figure 4.10** : O/P ratio of Mn, Zn and Cu promoted catalysts at 340 °C, 10 bar,  $H_2/CO = 1$ ,  $GHSV=2000 h^{-1}$ .

Light olefins yield of 10Fe2Mn, 10Fe2Zn and 10Fe-2Cu catalysts were plotted in Figure 4.11 and they were  $1.8 \times 10^{-3}$ ,  $0.8 \times 10^{-3}$  and  $0.6 \times 10^{-3} g_C/g_{Fe.s}$ , respectively. Mn produced more olefin product than Zn and Cu. Although CO conversions of Mn and Cu promoted catalysts were the same (Figure 4.9 (a)), Mn had highest olefin selectivity and olefin yield. Torres et al. [51] reported that the light olefins yield of 6 wt.% Fe/ $\alpha$ - $Al_2O_3$  catalyst was  $3.5 \times 10^{-4} g_C/g_{Fe.s}$  after 64 h reaction. Light olefins yield of 10Fe2Mn reached to  $0.6 \times 10^{-3} g_C/g_{Fe.s}$  in Figure 4.11. These results indicate olefin yield of 10Fe2Mn was higher than the olefin yield reported in literature [51].

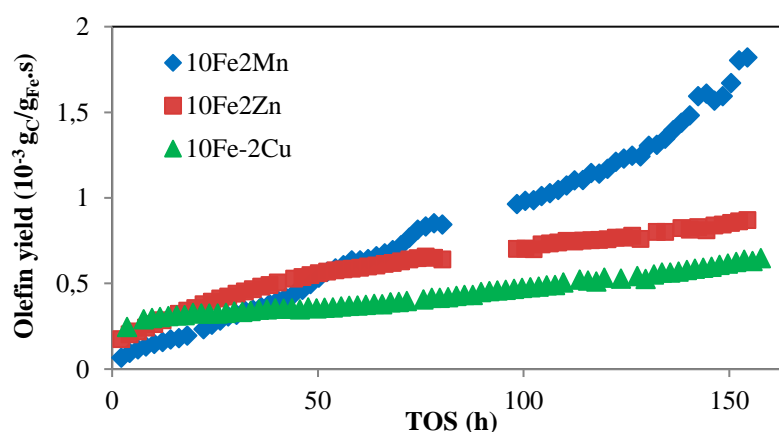


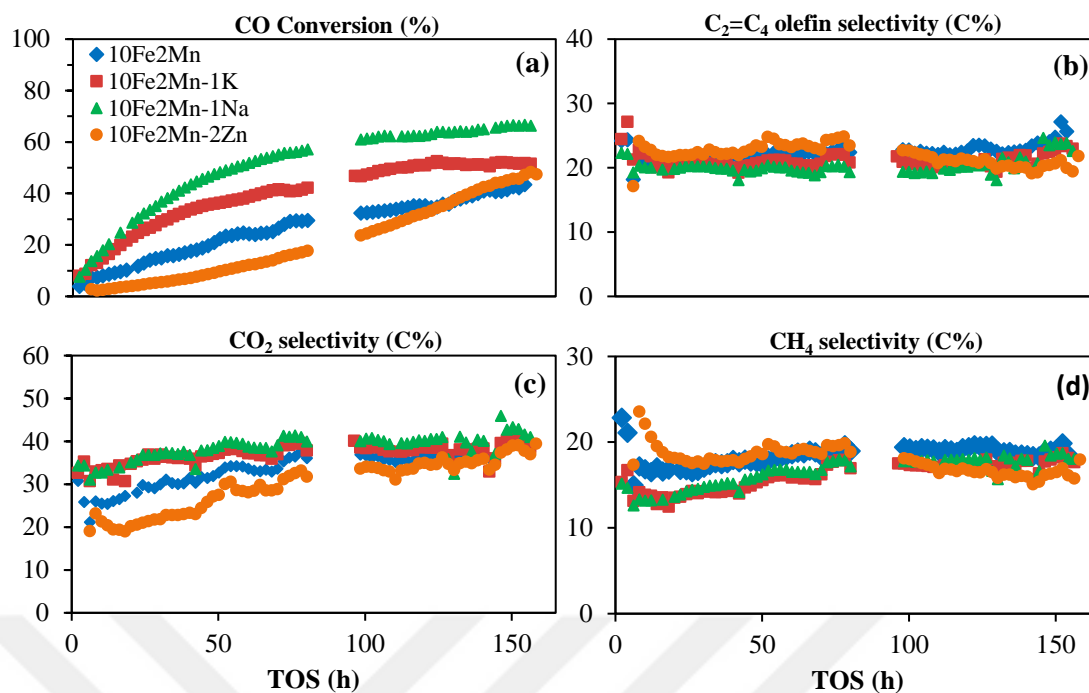
**Figure 4.11** : Light olefins yield of 10Fe2Mn, 10Fe2Zn and 10Fe-2Cu.

The best catalyst was 10Fe2Mn among these catalysts according to its olefin selectivity and olefin yield.

Next step was secondary promoting of 10Fe2Mn, 10Fe2Zn and 10Fe-2Cu to improve catalyst performance for FTO reaction.

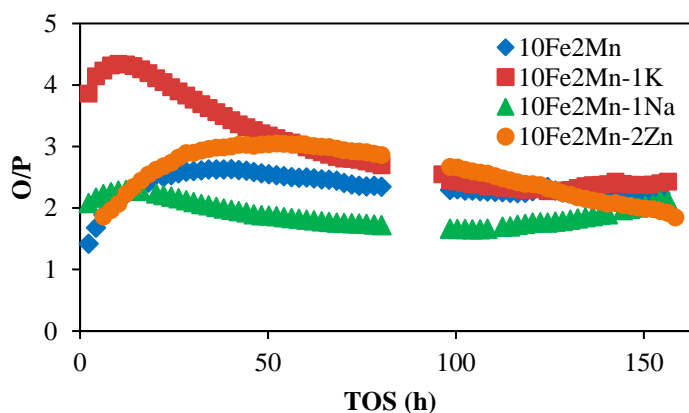
#### 4.2.5 Promoter effects of Zn, K and Na on 10Fe2Mn

Zn (2 wt.%), K (1 wt.%) and Na (1 wt.%) promoters were added to 10Fe2Mn catalyst to improve conversion and the selectivity to light olefins. Figure 4.12 shows (a) CO conversion, (b) light olefins, (c) CO<sub>2</sub> and (d) CH<sub>4</sub> selectivity of catalysts. Figure 4.12 (a) shows CO conversion of 10Fe2Mn and Zn, K and Na promoted 10Fe2Mn. CO conversion of 10Fe2Mn catalyst was 45% at the end of reaction. K additive on 10Fe2Mn improved CO conversion (51%) and stability of the catalyst as it is seen in Figure 4.12 (a). A higher CO conversion in presence of K is in agreement with the study of Wan et al. [47]. They found that addition of K promoter resulted in increase in the FT activity and improved the catalyst stability. Also, Tian et al. [14] synthesized Fe-MnK-AC catalysts and found that K promoter also favors of Fe carbides formation which increases CO conversion. Highest CO conversion was observed on 10Fe2Mn-1Na by 66%. Xiong et al. [37] observed that Na addition on CNT supported Fe catalysts resulted in increase of CO conversion. Addition of K and Na enhanced the conversion because they are alkali metals that enhance the surface basicity and facilitate the adsorption of CO. Olefin selectivity values of all catalysts were approximately 20% as it is seen in Figure 4.12 (b). Zn addition led to low CO<sub>2</sub> selectivity for the first 80 h of the reaction but K and Na additives led increase in CO<sub>2</sub> selectivity as it seen in Figure 4.12 (c). CO<sub>2</sub> selectivity values of all catalysts reached approximately 39% after 160 h. Tian et al. [14] reported that CO<sub>2</sub> selectivity values of different amounts of K and Mn combinations on AC support was between 45-48% which was similar value with the result of 10Fe2Mn-1K catalyst. CH<sub>4</sub> selectivity values were approximately 18% for all catalysts as shown in Figure 4.12 (d). As a conclusion, addition of Zn, K and Na promoters to 10Fe2Mn catalyst mainly had effect on the conversion but did not improve the selectivity to light olefins as it is seen in Figure 4.12 (a) and (b).



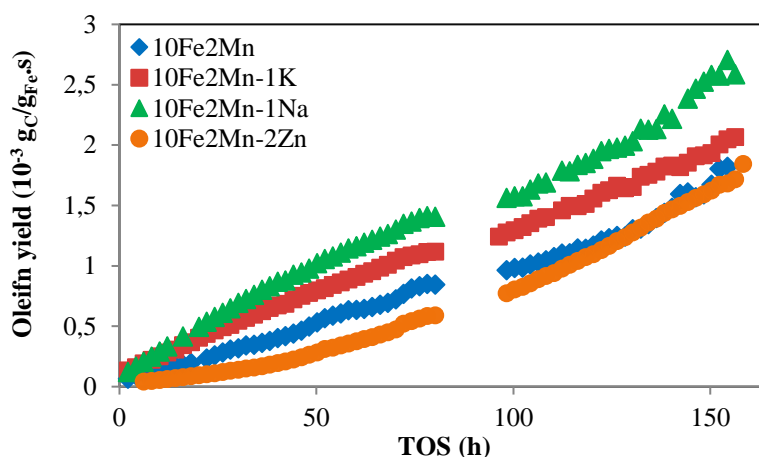
**Figure 4.12 :** (a) CO conversion, (b) light olefins, (c) CO<sub>2</sub> and (d) CH<sub>4</sub> selectivity of promoted 10Fe<sub>2</sub>Mn catalysts at 340 °C, 10 bar, H<sub>2</sub>/CO = 1, GHSV=2000 h<sup>-1</sup>.

Figure 4.13 shows how of Zn, K and Na additives affect the O/P ratio of 10Fe<sub>2</sub>Mn. O/P ratio of 10Fe<sub>2</sub>Mn-1K reached 4.3 after 12 h reaction period but then decreased slightly to 2.4. Tian et al. [14] reported that O/P ratio of Fe-MnK-AC (10.1 wt.% Fe, 29.3 wt.% Mn and 5.32 wt.% K) catalyst was 4.88 for 100 h reaction. This difference can be attributed to different amounts of Mn and K in two catalysts. Although, 10Fe<sub>2</sub>Mn-1Na had the highest conversion, average O/P ratio was 1.5. 10Fe<sub>2</sub>Mn-2Zn reached a maximum value 3.0 then decreased to 1.8 after 160 h.



**Figure 4.13 :** O/P ratio of promoted 10Fe<sub>2</sub>Mn catalysts at 340 °C, 10 bar, H<sub>2</sub>/CO = 1, GHSV=2000 h<sup>-1</sup>.

Figure 4.14 shows the light olefins yield of 10Fe<sub>2</sub>Mn and Zn, K and Na promoted 10Fe<sub>2</sub>Mn catalysts. K and Na promoters had a positive effect on olefin yield. Addition of Na improved the olefin yield of 10Fe<sub>2</sub>Mn from 1.8x10<sup>-3</sup> to 2.6x10<sup>-3</sup> gC/gFe.s. Olefin yield of 10Fe<sub>2</sub>Mn-1K reached 2.0x10<sup>-3</sup> gC/gFe.s at the end of the reaction. Addition of Zn reduced the olefin yield of 10Fe<sub>2</sub>Mn catalyst slightly. The light olefins yield of the catalysts in this group are higher than the reported yield for 64 h reaction [51].



**Figure 4.14 :** Light olefins yield of 10Fe<sub>2</sub>Mn, 10Fe<sub>2</sub>Mn-1K, 10Fe<sub>2</sub>Mn-1Na and 10Fe<sub>2</sub>Mn-2Zn.

Focusing on the olefin selectivity and low CH<sub>4</sub> selectivity, there was no significant difference between 10Fe<sub>2</sub>Mn-1K and 10Fe<sub>2</sub>Mn-1Na catalysts. The olefin yield of 10Fe<sub>2</sub>Mn-1Na was slightly higher than the olefin yield of 10Fe<sub>2</sub>Mn-1K. However, O/P ratio of 10Fe<sub>2</sub>Mn-1K was significantly higher than O/P ratio of 10Fe<sub>2</sub>Mn-1Na during 160 h reaction. So, 10Fe<sub>2</sub>Mn-1K was the best catalyst in this group.

#### 4.2.6 Promoter effects of Mn, K and Na on 10Fe<sub>2</sub>Zn

Mn (2 wt.%), K (1 wt.%) and Na (1 wt.%) promoters were introduced to 10Fe<sub>2</sub>Zn catalyst by the method described in Chapter 3. In Figure 4.15, (a) CO conversion, (b) light olefins, (c) CO<sub>2</sub> and (d) CH<sub>4</sub> selectivity of catalysts are shown. Figure 4.15 (a) shows that addition of K and Na did not have a significant effect on CO conversion of 10Fe<sub>2</sub>Zn catalyst. CO conversion was suppressed in the presence of Mn in 10Fe<sub>2</sub>Zn-2Mn. CO conversion of 10Fe<sub>2</sub>Zn reached 64% while the conversion of 10Fe<sub>2</sub>Zn-2Mn was 39% after 160 h. In Figure 4.15 (b) the light olefins selectivity of 10Fe<sub>2</sub>Zn was around 15%. It increased from 15% to approximately 24% by addition of Mn and Na

promoters. K promoted 10Fe2Zn catalyst improved the light olefins selectivity to 28% where it was almost 50% higher than the light olefins selectivity of 10Fe2Zn. Figure 4.15 (c) shows that CO<sub>2</sub> selectivity of each catalyst reached 40% at the end of the reaction period. As it is seen in Figure 4.15 (d) 10Fe2Zn-1K had the lowest CH<sub>4</sub> selectivity among other catalysts. CH<sub>4</sub> selectivity of Mn and Na promoted catalysts almost reached 20% whereas K promoted was 13% after 160 h.

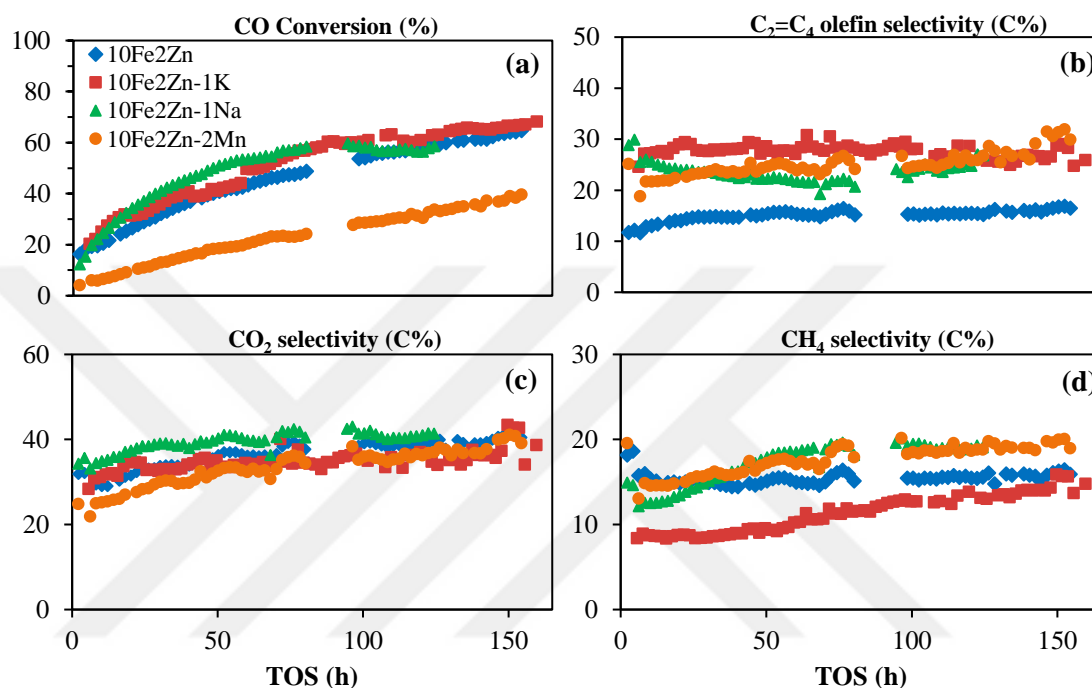


**Figure 4.15 :** (a) CO conversion, (b) light olefins, (c) CO<sub>2</sub> and (d) CH<sub>4</sub> selectivity of promoted 10Fe2Zn catalyst at 340 °C, 10 bar, H<sub>2</sub>/CO = 1, GHSV=2000 h<sup>-1</sup>.

Figure 4.16 shows O/P ratio of Mn, K and Na promoted 10FeZn catalyst. O/P ratio of 10Fe2Zn was approximately 1.0. It is seen that in Figure 4.16, addition of promoters had a positive effect on O/P ratio. Addition of Mn promoter to 10Fe2Zn increased O/P ratio to 2.8 at the end of the reaction. This result is the affirmation of the positive effect of Mn on olefin production by suppressing the C<sub>2</sub>-C<sub>4</sub> paraffins [13]. 10Fe2Zn-1K had a high initial O/P ratio about 5.6 but it was unstable and it decreased to 2.7. Na promoted catalyst showed an interesting trend. In the first hours of the reaction it was decreasing (from 3.1 to 1.6) but then it started to increase (from 1.6 to 2.9). Zhao et al. [49] tested co-precipitated bulk Fe-Zn-Na (Fe/Zn = 1/1, 1.86 wt.% Na) catalyst and reported that O/P ratio of catalyst was 6.91 for 12 h reaction. It was higher than O/P ratio of 10Fe2Zn-1Na catalyst in this study. This can be caused by the different

amounts of active metal and promoter, different synthesis methods of catalysts and using a different type of catalysts (bulk vs. AC supported).

Also, 10Fe2Zn-1Na catalyst exhibited the same trend with 10Fe2Mn-1Na catalyst in Figure 4.13.

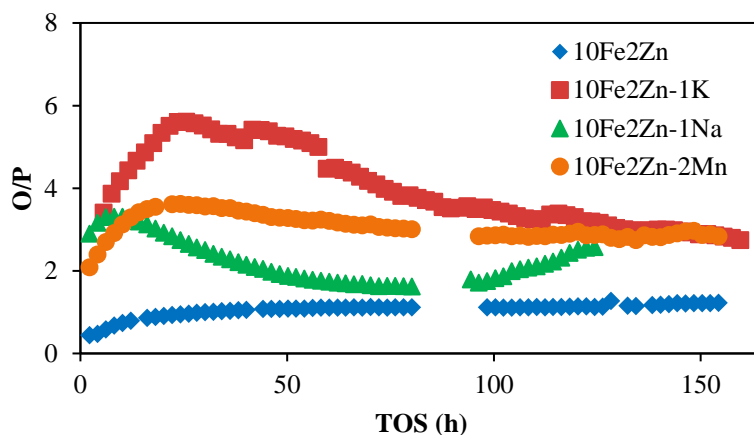


**Figure 4.16 :** O/P ratio of promoted 10Fe2Zn catalysts at 340 °C, 10 bar, H<sub>2</sub>/CO = 1, GHSV=2000 h<sup>-1</sup>.

The light olefins yield of 10FeZn and Mn, K and Na promoted 10Fe2Zn were plotted in Figure 4.17. In Figure 4.17, it is seen that addition of promoters on 10Fe2Zn enhanced the olefin yield. Olefin yield of Mn, K and Na promoted catalysts were  $2.1 \times 10^{-3}$ ,  $3.4 \times 10^{-3}$  and  $2.2 \times 10^{-3}$  g<sub>C</sub>/g<sub>Fe.s</sub> respectively. 10Fe2Zn-1K reached  $3.4 \times 10^{-3}$  g<sub>C</sub>/g<sub>Fe.s</sub> after 160 h which was the highest value among all catalysts. The light olefin yield of the catalysts in this group are higher than the reported olefin yield [51].

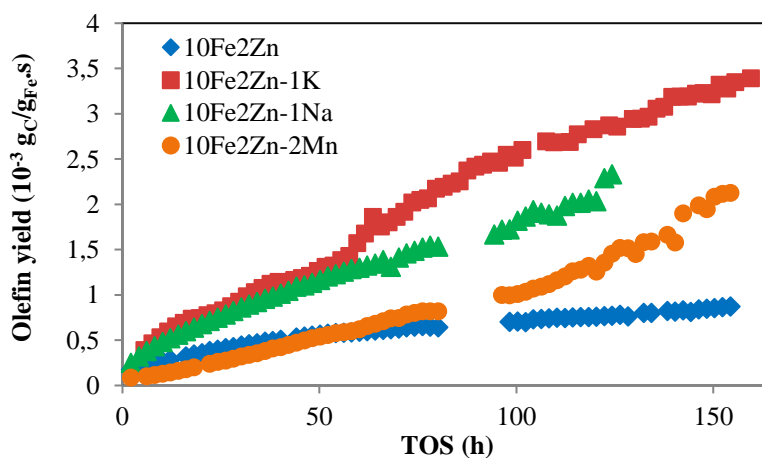


**Figure 4.17 :** Light olefins yield of 10Fe2Zn, 10Fe2Zn-2Mn, 10Fe2Zn-1K and 10Fe2Zn-1Na.

K and Na promoted 10Fe2Zn catalysts had high CO conversion. CH<sub>4</sub> selectivity of 10Fe2Zn-1K catalyst was lower than CH<sub>4</sub> selectivity of 10Fe2Zn-1Na catalyst. 10Fe2Zn-1K had higher selectivity to light olefins and higher O/P ratio than 10Fe2Zn-1Na during the reaction. Because of these reasons, 10Fe2Zn-1K catalyst was the best in this group.

#### **4.2.7 Promoter effect of Mn, Zn, K and Na on 10Fe-2Cu**

10Fe-2Cu, 10Fe-2Cu-2Mn, 10Fe-2Cu-2Zn, 10Fe-2Cu-1K and 10Fe-2Cu-1Na catalysts were synthesized by method described in Chapter 3. The effects of the promoters on CO conversion of 10Fe-2Cu catalyst are shown in Figure 4.18. CO conversion was improved in the presence of Mn, K and Na in 10Fe-2Cu as it is seen in Figure 4.18 (a). CO conversion of 10Fe-2Cu reached 47% after 160 h whereas 10Fe-2Cu-1K and 10Fe-2Cu-1Na and 10Fe-2Cu-2Mn reached to 57%, 64% and 53% respectively. An et al. [12] found that the addition of either K or Na enhances the surface basicity which affects the iron carbide formation and CO conversion. Zn addition on 10Fe-2Cu did not have a significant improvement on CO conversion. Addition of Mn, K and Na promoters also caused increase in selectivity of CO<sub>2</sub>. As it is seen in Figure 4.18 (c), addition of Mn, K and Na increased CO<sub>2</sub> selectivity of 10Fe-2Cu from 25% to approximately 30%. Bukur et al. [52] reported that both Cu and K promote the WGS activity of the catalyst, with K being the more effective promoter which was consistent with CO<sub>2</sub> selectivity value of 10Fe-2Cu-1K. However, CO<sub>2</sub> selectivity of 10Fe-2Cu reached the same value with Mn, K and Na promoted catalysts after 140 h. Figure 4.18 (b) shows that K and Na promoted catalysts had a higher olefin selectivity, c.a. 27%, than the other catalysts. CH<sub>4</sub> selectivity of alkali promoted catalysts were below 10% for 50 h of reaction but then it increased slightly to 13% at the end of the test as it is seen in Figure 4.18 (d). An et al. [12] reported that K and Na can suppress the formation of CH<sub>4</sub> and enhance the selectivity to olefins which are in agreement with this study. CH<sub>4</sub> selectivity of Mn promoted catalyst was approximately 20% while CH<sub>4</sub> selectivity of Zn promoted catalyst decreased from 20% to 13%. Addition of Zn on 10Fe-2Cu did not have any significant effect on CO conversion, CO<sub>2</sub> and light olefins selectivity.

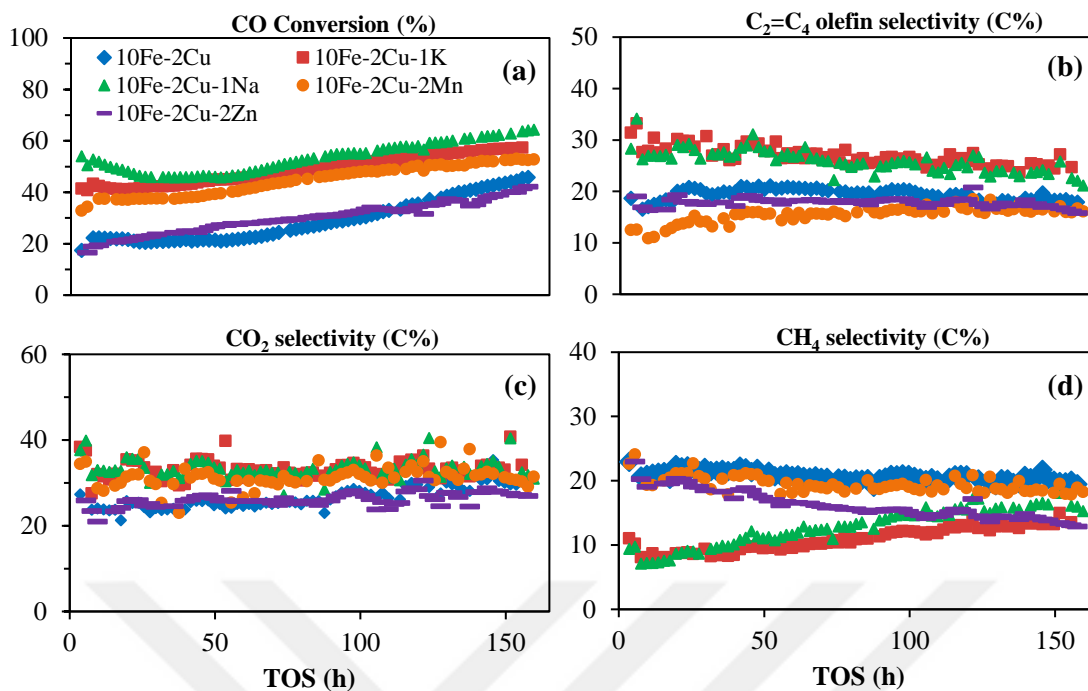


**Figure 4.18 :** (a) CO conversion, (b) light olefins, (c) CO<sub>2</sub> and (d) CH<sub>4</sub> selectivity of promoted 10Fe-2Cu catalysts at 340 °C, 10 bar, H<sub>2</sub>/CO = 1, GHSV=2000 h<sup>-1</sup>.

As reported in several articles addition of K to Cu promoted Fe based catalysts leads to low paraffin production during the reaction and this results in higher O/P ratios [39, 47]. K promoted catalyst, 10Fe-2Cu-1K, exhibited the highest O/P ratio among all other catalysts in Figure 4.19. O/P ratio reached 6.3 at the initial period of the reaction. This value was approximately seven times higher than the O/P ratio of 10Fe-2Cu. Then, it decreased to 3.8 after 160 h reaction. But still, it had the highest O/P ratio. Na promoted catalyst also showed a high O/P ratio (5.1) after 12 h reaction. But it decreased to 2.2 at the end of the reaction. O/P ratio of Zn promoted catalyst was 1.8 after 160 h. It is seen that Mn addition to 10Fe-2Cu catalyst did not improve O/P ratio in Figure 4.19.



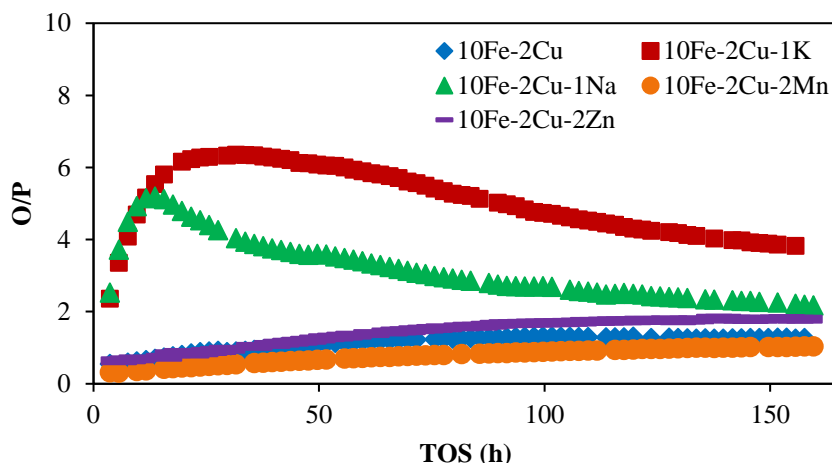


**Figure 4.19 :** O/P ratio of promoted 10Fe-2Cu catalysts at 340 °C, 10 bar,  $H_2/CO = 1$ ,  $GHSV=2000 h^{-1}$ .

Figure 4.20 shows that the light olefins yield of 10Fe-2Cu and Mn, Zn, K and Na promoted 10Fe-2Cu catalysts. K and Na addition on 10Fe-2Cu increased the olefin yield significantly. The light olefins yield of 10Fe-2Cu was  $0.6 \times 10^{-3} g_C/g_{Fe.s}$ , it reached  $1.0 \times 10^{-3} g_C/g_{Fe.s}$  after addition of K and Na as it is seen in Figure 4.20. Mn and Zn addition did not affect olefin yield as much as K and Na. Also, olefin yield of catalysts except 10Fe-2Cu for 64 h reaction are higher than the olefin yield that was reported in literature [51].

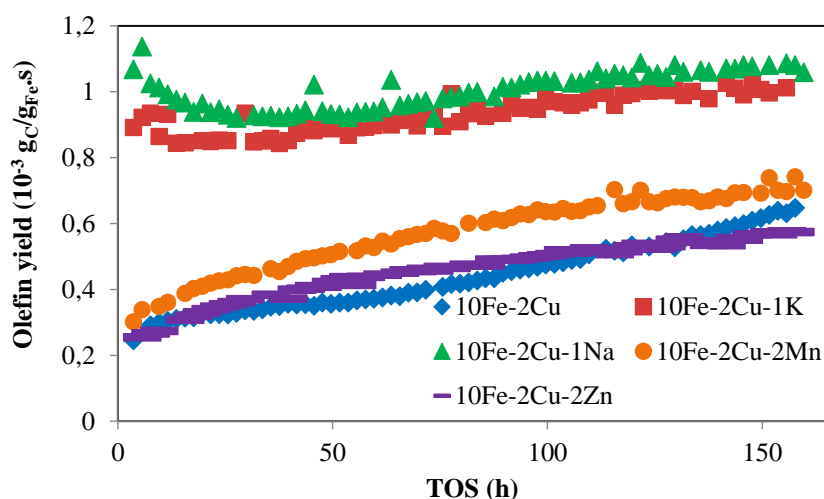


**Figure 4.20 :** Light olefins yield of 10Fe-2Cu, 10Fe-2Cu-1K, 10Fe-2Cu-1Na, 10Fe-2Cu-2Mn, 10Fe-2Cu-2Zn.

As a conclusion, 10Fe-2Cu-1K and 10Fe-2Cu-1Na catalysts exhibited similar performance for FTO reaction which is better than other catalysts. However, 10Fe-

2Cu-1K catalysts had a higher O/P ratio than 10Fe-2Cu-1Na catalyst. So, 10Fe-2Cu-1K catalyst was the best catalyst in this group.

#### 4.2.8 Promoter effects of Na and S promoters on AC supported Fe catalyst

Na and S promoters have been studied to produce light olefins in literature [16, 17, 42]. Oschatz et al. [17] studied Na and S promoters on carbon black support for FTO and optimum loadings were reported as 1-3 wt.% Na and 0.5-1 wt.% S with respect to iron. They tested catalysts at 340 °C, 10 bar and  $H_2/CO = 2$ . In this study, Na and S were loaded 3 wt.% and 1 wt.% with respect to Fe, referring to the study of Oschatz et al. [17]. Unlike Oschatz et al. [17] study, 10Fe0.3Na0.1S catalyst was tested at  $H_2/CO = 1$ . CO conversion and light olefins selectivity of 10Fe0.3Na0.1S were plotted in Figure 4.21. According to test results, in Figure 4.21 (a), CO conversion of catalyst lost activity until 60 h afterward CO conversion started to increase, in the end it reached approximately 30%. Figure 4.21 (b) shows that light olefins selectivity decreased slightly from 27% to 18%.

Oschatz et al. [17] achieved above 60% selectivity to light olefins but it was obtained between 20-30% in this study. The difference in the selectivity can be caused by low  $H_2/CO = 1$  ratio which was used in this study. Also, support material properties could affect the selectivity since Oschatz et al. [17] used carbon black whereas activated carbon was used in this study.

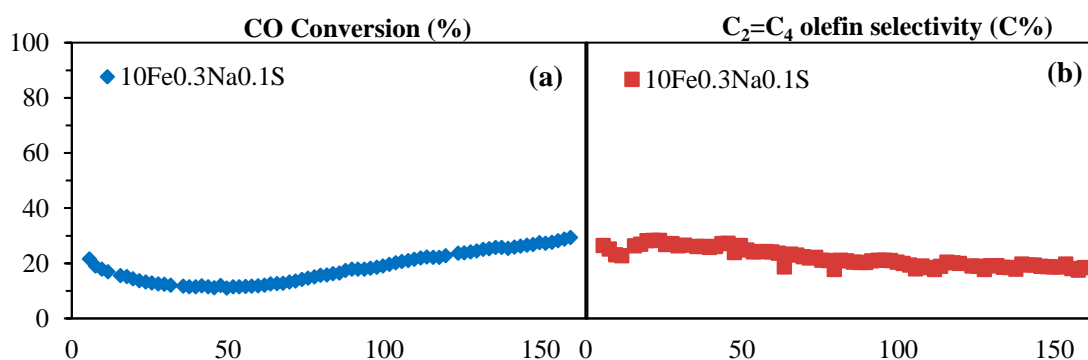


**Figure 4.21 :** (a) CO conversion and (b) light olefins selectivity of 10Fe0.3Na0.1S at 340 °C, 10 bar,  $H_2/CO = 1$ , GHSV=2000 h<sup>-1</sup>.

Figure 4.22 shows the O/P ratio of 10Fe0.3Na0.1S catalyst. O/P ratio was around 2.0 and lower than the other catalysts such as 10Fe2Zn-1K, 10Fe-2Cu-1K.

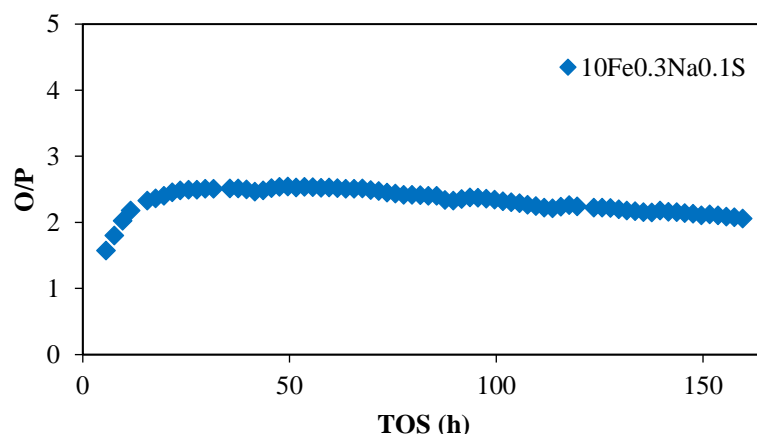


**Figure 4.22 :** O/P ratio of 10Fe0.3Na0.1S catalyst at 340 °C, 10 bar, H<sub>2</sub>/CO = 1, GHSV=2000 h<sup>-1</sup>.

As a conclusion, 10Fe0.3Na0.1S catalyst was not suitable to produce light olefins because of the low selectivity to light olefins and low O/P ratio.

#### 4.2.9 Comparison of 10Fe2Mn-1K, 10Fe2Zn-1K and 10Fe-2Cu-1K

According to all test results, 10Fe2Mn-1K, 10Fe2Zn-1K and 10Fe-2Cu-1K catalysts were the best catalysts considering higher CO conversion, higher selectivity to light olefins, lower CH<sub>4</sub> selectivity, O/P ratio and olefin yield. Figure 4.23 shows CO conversion, CO<sub>2</sub>, CH<sub>4</sub> and light olefins selectivity of 10Fe2Mn-1K, 10Fe2Zn-1K and 10Fe-2Cu-1K catalysts. Figure 4.23 (a) shows that CO conversion of 10Fe2Zn-1K was the highest with 68%. CO conversion of 10Fe-2Cu-1K had higher initial activity in the presence of Cu [18, 39]. 10Fe2Mn-1K was reached almost the same conversion as 10Fe-2Cu-1K. In Figure 4.23 (b) selectivity to light olefins of 10Fe2Mn-1K, 10Fe2Zn-1K and 10Fe-2Cu-1K was approximately 20%, 28% and 27% respectively. CO<sub>2</sub> selectivity values of catalysts were changed between 30-40% as it is seen in Figure 4.23 (c). Figure 4.23 (d) shows the CH<sub>4</sub> selectivity of catalysts. CH<sub>4</sub> selectivity of 10Fe2Mn-1K was 18%. CH<sub>4</sub> selectivity values of 10Fe2Zn-1K and 10Fe-2Cu-1K were approximately 13% after 160 h as it is seen in Figure 4.23 (d).

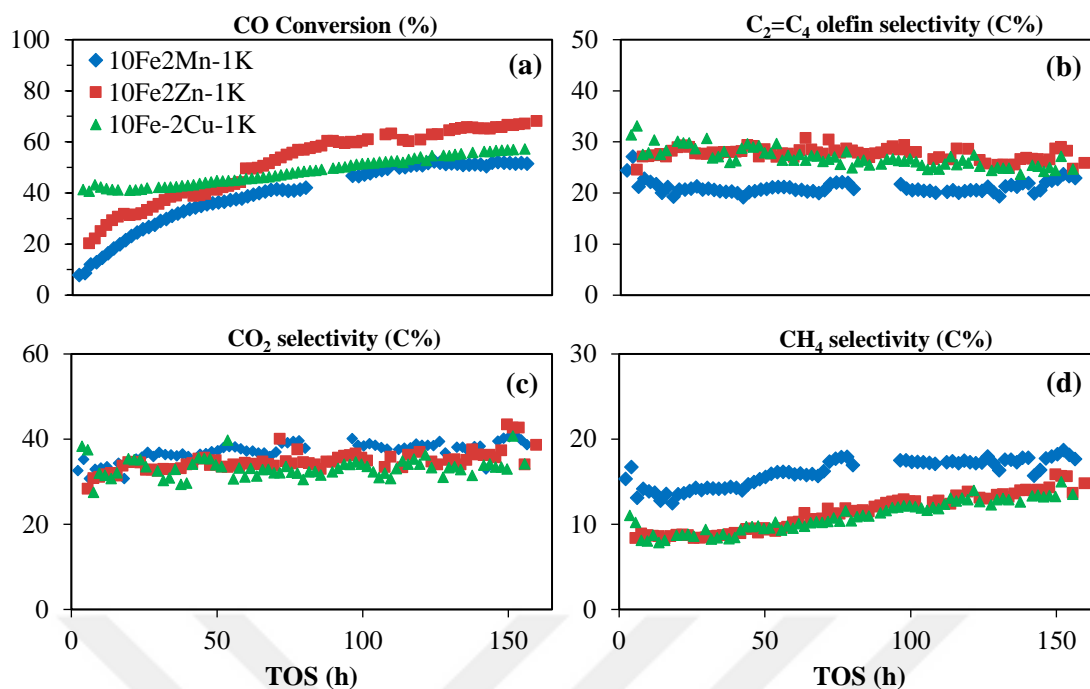


**Figure 4.23 :** (a) CO conversion, (b) light olefins, (c) CO<sub>2</sub> and (d) CH<sub>4</sub> selectivity of K promoted Mn, Zn and Cu catalysts at 340 °C, 10 bar, H<sub>2</sub>/CO = 1, GHSV=2000 h<sup>-1</sup>.

O/P ratios of 10Fe2Mn-1K, 10Fe2Zn-1K and 10Fe-2Cu-1K catalysts are plotted in Figure 4.24. Combination of Cu-K on AC supported Fe catalyst had the highest O/P ratio with a value 6.3 among three catalysts after 25 h reaction. Then, O/P ratio of 10Fe-2Cu-1K decreased to 3.8. At that time, O/P ratio of 10Fe2Zn-1K was 5.6 then it decreased to 2.7. The maximum value of O/P ratio of 10Fe2Mn-1K catalyst was 4.3 but then O/P ratio stabilized at 2.4.

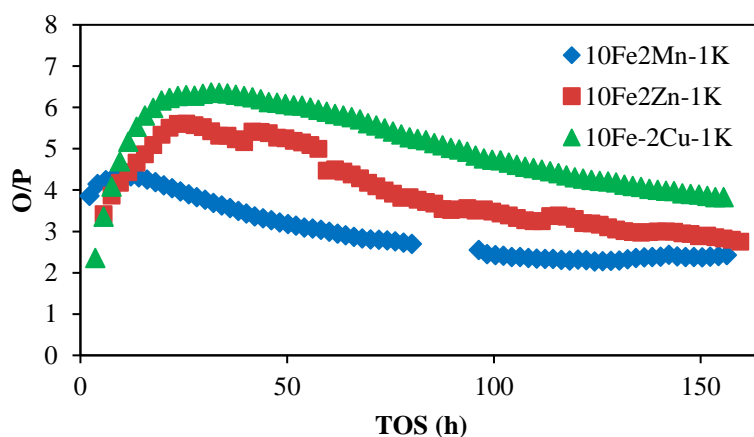


**Figure 4.24 :** O/P ratio of K promoted Mn, Zn and Cu catalysts at 340 °C, 10 bar, H<sub>2</sub>/CO = 1, GHSV=2000 h<sup>-1</sup>.

Figure 4.25 shows the light olefins yield of 10Fe2Mn-1K, 10Fe2Zn-1K and 10Fe-2Cu-1K catalysts. Olefin yield values were  $2.0 \times 10^{-3}$ ,  $3.4 \times 10^{-3}$  and  $1.0 \times 10^{-3}$  gC/gFe.s respectively at the end of the reaction. 10Fe2Zn-1K produced more olefin than 10Fe2Mn-1K and 10Fe-2Cu-1K catalysts even among 16 catalysts. The light olefins yield of 10Fe2Zn-1K was much more higher than reported in literature [51].

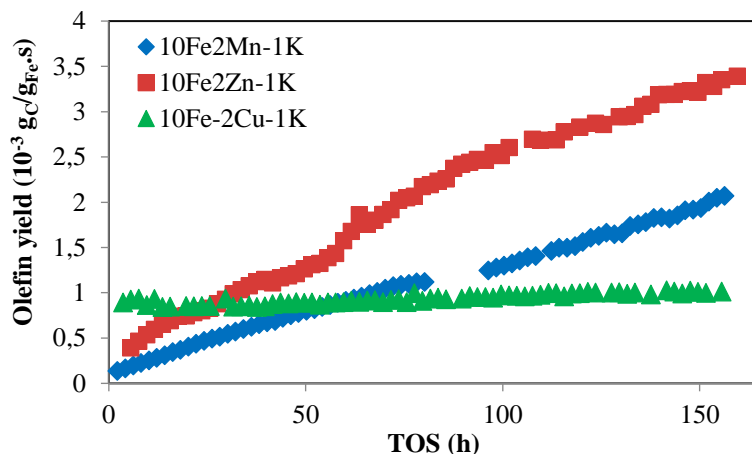


**Figure 4.25 :** Light olefins yield of 10Fe2Mn-1K, 10Fe2Zn-1K and 10Fe-2Cu-1K.

CO conversion, CO<sub>2</sub> selectivity, product selectivity, O/P ratio and the light olefins yield of 10Fe2Mn-1K, 10Fe2Zn-1K and 10Fe-2Cu-1K catalysts are given in Table 4.3. CO conversion values of catalysts were in order of increasing 10Fe2Mn-1K < 10Fe-2Cu-1K < 10Fe2Zn-1K which were in the same order of increasing surface areas. Surface area of 10Fe2Mn-1K, 10Fe-2Cu-1K and 10Fe2Zn-1K catalysts were 488.2, 651.9 and 664.7 m<sup>2</sup>/g. The higher surface area can be resulted in higher CO conversion. Because higher surface area helps the active metal distribution on support. Thus active sites are being more accessible by syngas.

In Table 4.3, 10Fe2Zn-1K had the highest CO<sub>2</sub> selectivity Zn promoter was reported as increase WGS activity [50]. The light olefins selectivity values of 10Fe2Zn-1K and 10Fe-2Cu-1K catalysts were close to each other (27.1 and 28.2%) whereas light olefins selectivity of 10Fe2Mn-1K was the lowest (22.9 %). Cu-K combination had the lowest C<sub>2</sub>-C<sub>4</sub> paraffin selectivity than other combinations. However, 10Fe-2Cu-1K produced more C<sub>5+</sub> (51.9 %) hydrocarbons. At the end of the reaction, O/P ratio of 10Fe-2Cu-1K catalyst was higher than other catalysts. The light olefins yield of Zn-K ( $3.4 \times 10^{-3}$  gC/gFe.s) combination was the highest. 10Fe2Zn-1K led to higher olefin yield while 10Fe-2Cu-1K led to higher O/P ratio.

**Table 4.3** : Catalytic performance of 10Fe2Mn-1K, 10Fe2Zn-1K and 10Fe-2Cu-1K.

Catalyst	CO Conversion (%)	CO <sub>2</sub> selectivity (C%)	Product selectivity (C%-CO <sub>2</sub> free)				O/P	C <sub>2</sub> =C <sub>4</sub> yield (x10 <sup>-3</sup> gC/gFe.s)
			CH <sub>4</sub>	C <sub>2</sub> -C <sub>4</sub>	C <sub>2</sub> =C <sub>4</sub>	C <sub>5</sub> +		
10Fe2Mn-1K	51.6	38.7	17.6	9.5	22.9	50.0	2.4	2.0
10Fe2Zn-1K	68.2	40.5	13.2	10.3	28.2	48.3	2.7	3.4
10Fe-2Cu-1K	57.3	30.7	13.9	7.1	27.1	51.9	3.8	1.0

Reaction conditions: 340 °C, 10 bar, H<sub>2</sub>/CO = 1, GHSV 2000 h<sup>-1</sup>, TOS 160 h.

According to high selectivity to light olefins and low selectivity to CH<sub>4</sub>, 10Fe2Zn-1K and 10Fe-2Cu-1K catalysts had better performance than 10Fe2Mn-1K catalyst. 10Fe2Zn-1K showed higher activity and olefin yield in this group. 10Fe-2Cu-1K showed a better O/P ratio. So, 10Fe2Zn-1K and 10Fe-2Cu-1K are the best catalysts among all catalysts.

## 5. CONCLUSION

In this study, AC supported Fe catalysts promoted with Mn, Zn, Cu, K, Na and S were synthesized for light olefins production from syngas by FTO process and investigated the effects of promoters on catalyst performances.

Catalysts were prepared by incipient wetness impregnation (IWI) method and tested in high throughput system in a fixed bed reactor. CO conversion, selectivity to CO<sub>2</sub>, CH<sub>4</sub>, light olefins (C<sub>2</sub>=C<sub>4</sub>), C<sub>5+</sub> of catalysts was examined. Also, O/P ratio and light olefins product yield of catalysts were considered. The main conclusions are given below.

1. All catalysts exhibited catalytic activity for FTO and produced light olefins at 340 °C and 10 bar.
2. Temperature increase resulted in a higher selectivity to light olefins whereas pressure increase resulted in a lower selectivity to light olefins.
3. Mn addition to 10Fe, suppresses the further hydrogenation of olefins thus addition of Mn resulted in a higher selectivity to light olefins compared to Cu and Zn addition.
4. Separately addition of K and Na on 10FeMn and 10Fe-2Cu resulted in a higher CO conversion.
5. K promoter in 10Fe2Zn-1K and 10Fe-2Cu-1K, helped to lower C<sub>2</sub>-C<sub>4</sub> paraffin and CH<sub>4</sub> selectivity.
6. Addition of Mn and Zn as a second promoter did not exhibit high performance for FTO compared to the performance of K and Na as a second promoter.
7. This work clearly demonstrates that using 10Fe2Zn-1K as a catalyst for FTO is a good choice regarding a higher yield to light olefins, high selectivity to light olefins, low selectivity to CH<sub>4</sub> and C<sub>2</sub>-C<sub>4</sub> paraffin.
8. Regarding a higher O/P ratio, high selectivity to light olefins, low selectivity to CH<sub>4</sub> and C<sub>2</sub>-C<sub>4</sub> paraffin, 10Fe-2Cu-1K catalyst can be used industrial application of FTO.

As a conclusion, AC supported Fe catalysts, especially promoted with Zn, Cu and K could be promising choices for FTO reaction industrially.





## REFERENCE

- [1] **Torres Galvis, H. M., & de Jong, K. P.** (2013). Catalysts for Production of Lower Olefins from Synthesis Gas: A Review. *ACS Catalysis*, 3(9), 2130–2149.
- [2] **Torres Galvis, H. M.** (2013). *Direct Production Of Lower Olefins From Synthesis Gas Using Supported Iron Catalyst Directe productie van lagere olefines uit synthese gas met gedragen ijzerkatalysatoren ( met een samenvatting in het Nederlands )*. Utrecht Universiteit.
- [3] **Oschatz, M., Hofmann, J. P., van Deelen, T. W., Lamme, W. S., Krans, N. A., Hensen, E. J. M., & de Jong, K. P.** (2017). Effects of the Functionalization of the Ordered Mesoporous Carbon Support Surface on Iron Catalysts for the Fischer–Tropsch Synthesis of Lower Olefins. *ChemCatChem*, 9(4), 620–628.
- [4] **van de Loosdrecht, J., Botes, F. G., Ciobica, I. M., Ferreira, A., Gibson, P., Moodley, D. J., ... Niemantsverdriet, J. W.** (2013). Fischer–Tropsch Synthesis: Catalysts and Chemistry. In J. Reedijk & K. Poepelmeier (Eds.), *Comprehensive Inorganic Chemistry II: From Elements to Applications* (pp. 525–557). Elsevier.
- [5] **Cheng, K., Ordonsky, V. V., Virginie, M., Legras, B., Chernavskii, P. A., Kazak, V. O., ... Khodakov, A. Y.** (2014). Support effects in high temperature Fischer-Tropsch synthesis on iron catalysts. *Applied Catalysis A: General*, 488, 66–77.
- [6] **Sun, B., Xu, K., Nguyen, L., Qiao, M., & Tao, F. F.** (2012). Preparation and Catalysis of Carbon-Supported Iron Catalysts for Fischer-Tropsch Synthesis. *ChemCatChem*, 4(10), 1498–1511.
- [7] **Xiong, H., Moyo, M., Motchelaho, M. A. M., Jewell, L. L., & Coville, N. J.** (2010). Fischer–Tropsch synthesis over model iron catalysts supported on carbon spheres: The effect of iron precursor, support pretreatment, catalyst preparation method and promoters. *Applied Catalysis A: General*, 388(1–2), 168–178.
- [8] **Xu, J. D., Zhu, K. T., Weng, X. F., Weng, W. Z., Huang, C. J., & Wan, H. L.** (2013). Carbon nanotube-supported Fe-Mn nanoparticles: A model catalyst for direct conversion of syngas to lower olefins. *Catalysis Today*, 215, 86–94.
- [9] **Gao, X., Zhang, J., Chen, N., Ma, Q., Fan, S., Zhao, T., & Tsubaki, N.** (2016). Effects of zinc on Fe-based catalysts during the synthesis of light olefins from the Fischer-Tropsch process. *Cuihua Xuebao/Chinese Journal of Catalysis*, 37(4), 510–516.
- [10] **Arakawa, H., & Bell, A. T.** (1983). Effects of Potassium Promotion on the

Activity and Selectivity of Iron Fischer-Tropsch Catalysts. *Industrial and Engineering Chemistry Process Design and Development*, 22(1), 97–103.

- [11] **Ribeiro, M. C., Jacobs, G., Davis, B. H., Cronauer, D. C., Kropf, A. J., & Marshall, C. L.** (2010). Fischer - Tropsch Synthesis : An In-Situ TPR-EXAFS / XANES Investigation of the Influence of Group I Alkali Promoters on the Local Atomic and Electronic Structure of Carburized Iron / Silica Catalysts, 7895–7903.
- [12] **An, X., Wu, B., Wan, H.-J., Li, T.-Z., Tao, Z.-C., Xiang, H.-W., & Li, Y.-W.** (2007). Comparative study of iron-based Fischer–Tropsch synthesis catalyst promoted with potassium or sodium. *Catalysis Communications*, 8(12), 1957–1962.
- [13] **Asami, K., Komiyama, K., Yoshida, K., & Miyahara, H.** (2018). Synthesis of Lower Olefins from Synthesis Gas over Active Carbon-Supported Iron Catalyst. *Catalysis Today*, 303(June 2017), 117–122.
- [14] **Tian, Z., Wang, C., Si, Z., Ma, L., Chen, L., & Liu, Q.** (2017). Applied Catalysis A , General Fischer-Tropsch synthesis to light ole fi ns over iron-based catalysts supported on KMnO 4 modi fi ed activated carbon by a facile method. *Applied Catalysis A, General*, 541(January), 50–59.
- [15] **Cheng, Y., Lin, J., Xu, K., Wang, H., Yao, X., Pei, Y., ... Zong, B.** (2016). Fischer-Tropsch Synthesis to Lower Olefins over Potassium-Promoted Reduced Graphene Oxide Supported Iron Catalysts. *ACS Catalysis*, 6(1), 389–399.
- [16] **Torres, H. M., Koeken, A. C. J., Bitter, J. H., Davidian, T., Ruitenbeek, M., Dugulan, A. I., & Jong, K. P. De.** (2013). Effects of sodium and sulfur on catalytic performance of supported iron catalysts for the Fischer – Tropsch synthesis of lower olefins. *Journal of Catalysis*, 303, 22–30.
- [17] **Oschatz, M., Krans, N., Xie, J., & de Jong, K. P.** (2016). Systematic variation of the sodium/sulfur promoter content on carbon-supported iron catalysts for the Fischer–Tropsch to olefins reaction. *Journal of Energy Chemistry*, 25(6), 985–993.
- [18] **Schulz, H.** (1999). Short history and present trends of Fischer–Tropsch synthesis. *Applied Catalysis A: General*, 186(1–2), 3–12.
- [19] **EPCA.** (2016). Petrochemicals & EPCA - A Passionate Journey.
- [20] **IHS Markit.** (n.d.). Ethylene, Chemical Economics Handbook, 2019. Retrieved February 15, 2019, from <https://ihsmarkit.com/products/ethylene-chemical-economics-handbook.html>
- [21] **Garside, M.** (n.d.). Ethylene production in the United States from 1990 to 2018. Retrieved October 10, 2019, from <https://www.statista.com/statistics/974766/us-ethylene-production-volume/>
- [22] **Mar, J.** (2018). *Petrochemical Production Statistics Western Europe (EUI5+Norway)* ).
- [23] **IHS Markit.** (n.d.). Propylene, Chemical Economics Handbook. Retrieved November 1, 2019, from <https://ihsmarkit.com/products/propylene->

- [24] **Garside, M.** (n.d.). Propylene production in the United States from 1990 to 2018. Retrieved October 10, 2019, from <https://www.statista.com/statistics/974833/us-propylene-production-volume/>
- [25] **Chen, D., Moljord, K., & Holmen, A.** (2012). Microporous and Mesoporous Materials A methanol to olefins review : Diffusion , coke formation and deactivation on SAPO type catalysts. *Microporous and Mesoporous Materials*, 164, 239–250.
- [26] **Dong, X., Liu, C., Miao, Q., Yu, Y., & Zhang, M.** (2019). Comparison of catalytic performance of metal-modified SAPO-34: a molecular simulation study. *Journal of Molecular Modeling*, 25(9).
- [27] **Wang, C., Xu, L., & Wang, Q.** (2003). Review of Directly Producing Light Olefins via CO Hydrogenation. *Journal of Natural Gas Chemistry*, 12(1), 10–16.
- [28] **Janardanao, M.** (1990). Direct Catalytic Conversion of Synthesis Gas to Lower Olefins. *Industrial and Engineering Chemistry Research*, 29(9), 1735–1753.
- [29] **Mahmoudi, H., Mahmoudi, M., Doustdar, O., Jahangiri, H., Tsolakis, A., Gu, S., & LechWyszynski, M.** (2018). A review of Fischer Tropsch synthesis process, mechanism, surface chemistry and catalyst formulation. *Biofuels Engineering*, 2(1), 11–31.
- [30] **Jahangiri, H., Bennett, J., Mahjoubi, P., Wilson, K., & Gu, S.** (2014). A review of advanced catalyst development for Fischer–Tropsch synthesis of hydrocarbons from biomass derived syn-gas. *Catal. Sci. Technol.*, 4(8), 2210–2229.
- [31] **Dry, M. E.** (2002). The Fischer–Tropsch process: 1950–2000. *Catalysis Today*, 71(3–4), 227–241.
- [32] **Adesina, A. A.** (1996). Hydrocarbon synthesis via Fischer-Tropsch reaction: Travails and triumphs. *Applied Catalysis A: General*, 138(2), 345–367.
- [33] **van der Laan, G. P.** (1999). *Kinetics, Selectivity and Scale Up of the Fischer-Tropsch Synthesis*. University of Groningen.
- [34] **Khodakov, A. Y., Chu, W., & Fongarland, P.** (2007). Advances in the development of novel cobalt Fischer-Tropsch catalysts for synthesis of long-chain hydrocarbons and clean fuels. *Chemical Reviews*, 107(5), 1692–1744.
- [35] **Li, T., Wang, H., Yang, Y., Xiang, H., & Li, Y.** (2013). Effect of manganese on the catalytic performance of an iron-manganese bimetallic catalyst for light olefin synthesis. *Journal of Energy Chemistry*, 22(4), 624–632.
- [36] **Ma, W., Kugler, E. L., & Dadyburjor, D. B.** (2007). Potassium effects on activated-carbon-supported iron catalysts for Fischer-Tropsch synthesis. *Energy and Fuels*, 21(4), 1832–1842.
- [37] **Xiong, H., Motchelaho, M. A., Moyo, M., Jewell, L. L., & Coville, N. J.** (2015). Effect of Group i alkali metal promoters on Fe/CNT catalysts in

Fischer-Tropsch synthesis. *Fuel*, 150, 687–696.

- [38] **Zhao, X., Lv, S., Wang, L., Li, L., Wang, G., Zhang, Y., & Li, J.** (2018). Comparison of preparation methods of iron-based catalysts for enhancing Fischer-Tropsch synthesis performance. *Molecular Catalysis*, 449(November 2017), 99–105.
- [39] **Ma, W., Kugler, E. L., & Dadyburjor, D. B.** (2011). Promotional Effect of Copper on Activity and Selectivity to Hydrocarbons and Oxygenates for Fischer-Tropsch Synthesis over Potassium-Promoted Iron Catalysts Supported on Activated Carbon. *Energy & Fuels*, 25(5), 1931–1938.
- [40] **Bussemeier, B.** (1986). *U.S. Patent No. 4,564,642*. Washington, DC: U.S. Patent and Trademark Office.
- [41] **Cheng, K., Ordonsky, V. V., Legras, B., Virginie, M., Paul, S., Wang, Y., & Khodakov, A. Y.** (2015). Sodium-promoted iron catalysts prepared on different supports for high temperature Fischer-Tropsch synthesis. *Applied Catalysis A: General*, 502, 204–214.
- [42] **Oschatz, M., van Deelen, T. W., Weber, J. L., Lamme, W. S., Wang, G., Goderis, B., ... de Jong, K. P.** (2016). Effects of calcination and activation conditions on ordered mesoporous carbon supported iron catalysts for production of lower olefins from synthesis gas. *Catalysis Science & Technology*, 6(24), 8464–8473.
- [43] **Ma, W., Kugler, E. L., & Dadyburjor, D. B.** (2010). Effect of Properties of Various Activated-Carbon Supports and Supported Fe-Mo-Cu-K Catalysts on Metal Precursor Distribution, Metal Reduction, and Fischer-Tropsch Synthesis. *Energy & Fuels*, 24(8), 4099–4110.
- [44] **Zhang, J., Lu, S., Su, X., Fan, S., Ma, Q., & Zhao, T.** (2015). Selective formation of light olefins from CO<sub>2</sub> hydrogenation over Fe-Zn-K catalysts. *Journal of CO<sub>2</sub> Utilization*, 12, 95–100.
- [45] **Yang, Zhang, Liu, Ning, Han, Liu, & Huo.** (2019). Preparation of Iron Carbides Formed by Iron Oxalate Carburization for Fischer-Tropsch Synthesis. *Catalysts*, 9(4), 347.
- [46] **Gu, B., Ordonsky, V. V., Bahri, M., Ersen, O., Chernavskii, P. A., Filimonov, D., & Khodakov, A. Y.** (2018). Effects of the promotion with bismuth and lead on direct synthesis of light olefins from syngas over carbon nanotube supported iron catalysts. *Applied Catalysis B: Environmental*, 234(February), 153–166.
- [47] **Wan, H., Wu, B., Zhang, C., Xiang, H., & Li, Y.** (2008). Promotional effects of Cu and K on precipitated iron-based catalysts for Fischer-Tropsch synthesis. *Journal of Molecular Catalysis A: Chemical*, 283(1–2), 33–42.
- [48] **Zhang, C., Yang, Y., Tao, Z., Li, T., Wan, H., Xiang, H., & Li, Y.** (2006). Effects of Cu and K on Co-precipitated FeMn/SiO<sub>2</sub> Catalysts for Fischer-Tropsch Synthesis. *Acta Physico - Chimica Sinica*, 22(11), 1310–1316.
- [49] **Zhao, M., Yan, C., Jinchang, S., & Qianwen, Z.** (2018). Modified iron catalyst

for direct synthesis of light olefin from syngas. *Catalysis Today*, 316(February), 142–148.

- [50] **Wang, H., Yang, Y., Xu, J., Wang, H., Ding, M., & Li, Y.** (2010). Study of bimetallic interactions and promoter effects of FeZn, FeMn and FeCr Fischer–Tropsch synthesis catalysts. *Journal of Molecular Catalysis A: Chemical*, 326(1–2), 29–40.
- [51] **Torres Galvis, H. M., Bitter, J. H., Khare, C. B., Ruitenbeek, M., Dugulan, A. I., & de Jong, K. P.** (2012). Supported Iron Nanoparticles as Catalysts for Sustainable Production of Lower Olefins. *Science*, 335(6070), 835–838.
- [52] **Bukur, D. B., Mukesh, D., & Patel, S. A.** (1990). Promoter effects on precipitated iron catalysts for Fischer-Tropsch synthesis. *Industrial & Engineering Chemistry Research*, 29(2), 194–204.





## CURRICULUM VITAE



**Name Surname** : Melis Kirarslan  
**Place and Date of Birth** : Silifke – 08.03.1993  
**E-Mail** : meliskirarslan@gmail.com

### EDUCATION :

- **B.Sc.** : 2017, Hacettepe University, Engineering Faculty, Chemical Engineering (English)
- **M.Sc.** : 2020, Istanbul Technical University, Chemical and Metallurgical Engineering Faculty, Chemical Engineering

### PROFESSIONAL EXPERIENCE AND REWARDS:

- 2019 TUBITAK MRC – Research Scholar

### PRESENTATION ON THE THESIS:

- **Kirarslan M., Gümüslü G. G., Behmenyar G.**, 2019: Catalyst Development for Light Olefins Production from Cleaned Syngas. Istanbul Technical University 1<sup>st</sup> Graduate Student Symposium, April 26, 2019 Istanbul, Turkey.